Inorganic Chemistry

Article

pubs.acs.org/IC

Iminopyridine Complexes of Manganese, Rhenium, and Molybdenum Derived from Amino Ester Methylserine and Peptides Gly-Gly, Gly-Val, and Gly-Gly-Gly: Self-Assembly of the Peptide Chains

Celedonio M. Álvarez, Raúl García-Rodríguez, and Daniel Miguel*

IU CINQUIMA/Química Inorgánica, Facultad de Ciencias, Universidad de Valladolid, E-47005 Spain

Supporting Information

ABSTRACT: Complexes containing pyridine-2-carboxaldehyde (pyca) ligand acting as κ^2-(N,O) chelates in $[MX(CO)_3(pyca)]$ (M = Mn, Re; X = Cl, Br), or $[MoX(methallyl)(CO)_2(pyca)]$ (X = Cl, Br), are good precursors for iminopyridine complexes derived from amino esters and peptides of formula $[MX(CO)_3(py\text{-}2\text{-}C(H){=}NCHX\text{-}COOY)]$ or $[MoX(methallyl)(CO)_2(py\text{-}2\text{-}C(H){=}NCHX\text{-}COOY)]$, via Schiff condensation of the aldehyde function of pyca with the terminal NH_2 group of the amino ester or peptide. X-ray determinations confirm the structures and show that in solid phase the peptide chains assemble through H-bonds adopting different patterns which depend on the geometry of the metal−ligand fragments. The H-bonding patterns have been analyzed in detail and described by using graph set methods. In most cases, Mo complexes show intramolecular arrangement involving the halogen (Cl or Br) and an NH group of the side chain. For the Mn and Re complexes, the peptide side arms form infinite chains, helices, and rings. In many cases, the terminal carboxylic O−H function is engaged in a "terminal" H-bond with a polar molecule of solvent (THF or acetone), instead of forming the usual head-to-head arrangement found in simple carboxylic acids. For the longer tripeptide Gly-Gly-Gly, a discrete, dimeric association is observed, in which the peptide chains show antiparallel arrangement with a complementary disposition of the internal N—H and C═O functions. DOSY experiments in solution show significant changes in the diffusion rates upon addition of $OPBu_3$, which indicate H-bonding interaction of $OPBu_3$ with the peptide hydrogens.

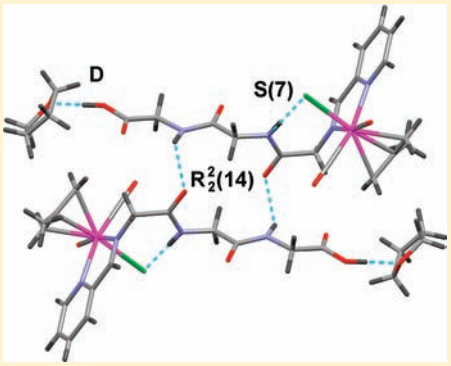

INTRODUCTION

There is a growing interest in the preparation of metal complexes containing peptide side arms, which can help to anchor them to a protein, thus introducing the metal fragment as a reporter group.[1,2] Moreover, such complexes may help to study the hydrogen-bond interactions responsible for the structure and, ultimately, the chemical and biological function of proteins.[3]

The incorporation of metal centers into proteins and polypeptides has facilitated the study of metalloprotein structures and biological electron-transfer mechanisms.[4] It has been reported recently that peptide-based phosphorus ligands are able to produce intramolecular self-assembly of the peptide chains when coordinated to a metal, forming β-turns[5] or antiparallel β-structures,[6] and the resulting complexes have been applied as asymmetric catalysts. Metal peptide nanoconjugates have been used for the preparation of gold and silver nanoparticles.[7]

Complexes having a pendant arm derived from an amino acid or amino ester have attracted the attention of several groups in the last few years as a convenient way to functionalize biological molecules.[8] Additionally, there is a sustained interest in the understanding and control of the organization of molecules in the crystalline state,[9] since the crystal packing of the molecules often determines bulk material properties such as magnetism, nonlinear optics, or conductivity. In this regard, control of hydrogen bonding has attracted much attention in the design of various molecular assemblies by virtue of the directionality and specificity. Ferrocene peptide conjugates have been used as convenient macromolecular building blocks for the construction of supramolecular structures via hydrogen bonding.[10] There are also several reports of the use of complexes containing iminopyridines derived from substituted phenols to study the solid-state arrangement due to H-bonding involving the OH groups.[11]

Previously we have reported complexes with iminopyridines derived from amino acids[12] and amino esters[13] which were found to exhibit a diversity of H-bonding arrangements in the solid state, and very recently, Herrick has reported dimeric iminopyridine complexes derived from glycine and alanine,[14] and a family of complexes of the $W(CO)_4$ fragment with iminopyridine derived from dipeptide-esters.[15] Thus, we considered to be of interest the introduction of additional hydroxyl or NH groups capable of establishing intermolecular interactions in the solid state. Following the pioneering work of Alberto et al.,[16] we have prepared complexes containing pyridine-2-carboxaldehyde acting as κ^2-(N,O) chelates, which are convenient precursors for iminopyridine complexes.

In this Article we report the preparation and characterization, including structural determinations, of new complexes of manganese, rhenium, and molybdenum with iminopyridine ligands bearing methylserine ester and dipeptide or tripeptide

Received: October 24, 2011
Published: February 13, 2012

   dx.doi.org/10.1021/ic2022984 | *Inorg. Chem.* 2012, 51, 2984−2996

pendant arms (Scheme 1), and the study of their H-bonding patterns in solid state and in solution.

Scheme 1. Synthesis of Iminopyridine Complexes Derived from Amino Ester, Dipeptide, or Tripeptide

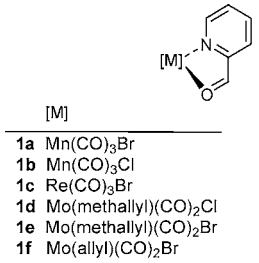

[M]	
1a	$Mn(CO)_3Br$
1b	$Mn(CO)_3Cl$
1c	$Re(CO)_3Br$
1d	$Mo(methallyl)(CO)_2Cl$
1e	$Mo(methallyl)(CO)_2Br$
1f	$Mo(allyl)(CO)_2Br$

[M]	R-COOR'
2a	$Mn(CO)_3Br$	$CH(CH_2OH)COOMe$
2d	$Mo(methallyl)(CO)_2Cl$	$CH(CH_2OH)COOMe$
3a	$Mn(CO)_3Br$	$CH_2CONHCH_2COOH$
3b	$Mn(CO)_3Cl$	$CH_2CONHCH_2COOH$
3c	$Re(CO)_3Br$	$CH_2CONHCH_2COOH$
3d	$Mo(methallyl)(CO)_2Cl$	$CH_2CONHCH_2COOH$
3e	$Mo(methallyl)(CO)_2Br$	$CH_2CONHCH_2COOH$
3f	$Mo(allyl)(CO)_2Br$	$CH_2CONHCH_2COOH$
4a	$Mn(CO)_3Br$	$CH_2CONHCH^iPrCOOH$
4c	$Re(CO)_3Br$	$CH_2CONHCH^iPrCOOH$
4d	$Mo(methallyl)(CO)_2Cl$	$CH_2CONHCH^iPrCOOH$
4e	$Mo(methallyl)(CO)_2Br$	$CH_2CONHCH^iPrCOOH$
5a	$Mn(CO)_3Br$	$CH_2CONHCH_2CONHCH_2COOH$
5c	$Re(CO)_3Br$	$CH_2CONHCH_2CONHCH_2COOH$
5d	$Mo(methallyl)(CO)_2Cl$	$CH_2CONHCH_2CONHCH_2COOH$

RESULTS AND DISCUSSION

Derivatives from L-Methylserine. Reactions of complexes containing pyridine-2-carboxaldehyde (pyca) ligand acting as κ^2-(N,O), **1a** or **1d**, with methylserine hydrochloride in the presence of a base gave derivatives **2a** or **2d** in good yields (see Scheme 2). The solid-state structures were confirmed by

Scheme 2. Synthesis of Iminopyridine Complexes Derived from the Amino Ester Methyl-L-Serine

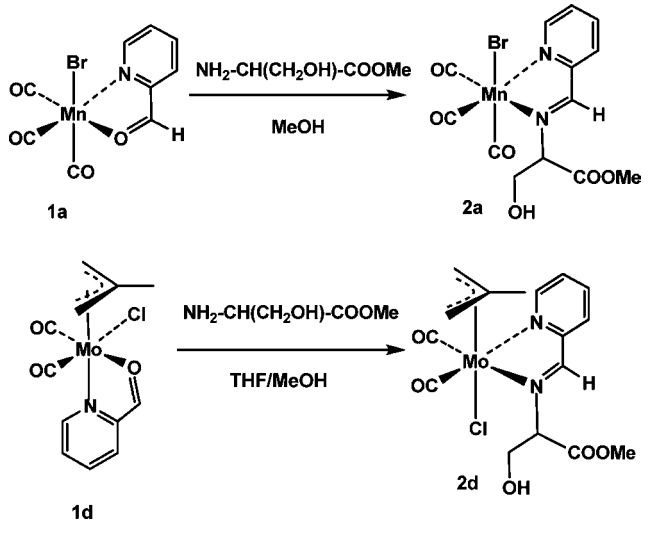

X-ray crystallography, showing interesting differences in their H-bonding pattern, which will be discussed below.

A detailed inspection of spectroscopic data reveals that the reactions with L-methylserine lead to the formation of two diastereoisomers, arising from the presence of two stereogenic centers: the α-carbon of the amino ester and the metal. ^{1}H NMR spectra of the crude reaction mixtures show a diastereoisomer ratio of 80/20. The crystal structure determinations **2a** and **2d** correspond to the major isomers, as confirmed by NMR analysis of samples of the crystals used for the X-ray studies. It has been suggested by Herrick et al. that the predominance of one diastereoisomer may be due to electronic interactions during the formation of the complex, when polar groups are present.[17] This is consistent with the observation of the high 80/20 ratio for the methylserine derivatives bearing a polar hydroxyl group. Interestingly, the presence of polar N−H and carboxylic groups in the peptide derivatives described below does not produce such high discrimination between the possible diastereoisomers.

The harsh conditions used for the formation of complexes **2a,d** produce racemization of the amino ester and, for **2a,** halide scrambling between the Br ligand and the chloride ion present in the starting amino ester hydrochloride salt. For the molybdenum complex **2d**, the racemization is complete, and both enantiomers are found in the crystal lattice, forming a centrosymmetric dinuclear arrangement through H-bonds (Figure 2). It has been proposed that the racemization is due to the presence of base.[17,18] In this case, where no strong base is present, the racemization can be attributed to the acidity of the hydrogen in C^α adjacent of the iminopyridine ligand (see below).

Reactions with Peptides. Complexes **1a−d** react with dipeptides to afford the corresponding iminopyridine derivatives **3a−d** (from Gly-Gly) and **4a−d** (from Gly-Val) as depicted in Scheme 3. A similar procedure using the tripeptide Gly-Gly-Gly affords complexes **5a−d**. The reactions can be carried out in refluxing methanol or ethanol, and require long refluxing times (see Experimental Section), probably due to the low solubility of the peptides. Despite the strong conditions, the complexes are produced in high yields and there is no racemization, as suggested by the crystallization of enantiopure Gly-Val derivative **4d**. This could be due to the low acidity of C^α valine proton compared to that of C^α adjacent to iminopyridine (see Scheme 4 below). Interestingly, in the case of **4d** it is the minor isomer which crystallizes out more easily from the mixture.

For the derivatives with Gly-Val, the NMR spectra of the crude reaction mixtures show the formation of diastereoisomers, arising from the presence of two stereogenic centers (the metal and the α-carbon of L-Val). In contrast with the serine amino ester derivatives **2a,d** described above, for compounds **4** there is no great discrimination between the two diastereoisomers: NMR spectra of molybdenum complex **4d** shows a ratio of 55/45 (vs 80/20 for the serine amino ester). For the rhenium complex **4c** the ratio is 48/52. The low solubility of manganese complexes, and the quadrupole effect, results in low-resolution spectra, thus precluding an accurate determination of the diastereoisomeric ratio for **4a** which, in any case, is not far from 50/50. The lack of discrimination between diastereoisomers in the complexes with peptides may be due to the fact that the polar NH group is two bonds further away from the metal when compared to the OH group of the serine derivatives.

Hydrogen Bonding Arrangement in Solid State. As could be anticipated, the presence of one hydroxyl group in the methylserine complexes **2a** and **2d** produces hydrogen bonding in the solid state, and the hydrogen bonding pattern depends greatly on the geometry of the derivative.

Thus, in the manganese complex **2a** there is only intramolecular Br···H−O bonding of type **S(7)** (Figure 1).[19]

dx.doi.org/10.1021/ic2022984 | Inorg. Chem. 2012, 51, 2984−2996

Scheme 3. Synthesis of Iminopyridine Complexes Derived from Peptides

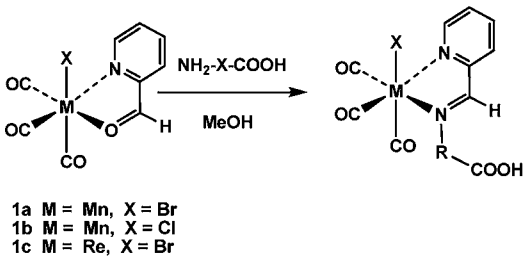

	M	X	Péptide	R
3a	Mn	Br	GlyGly	-$CH_2CONHCH_2$-
3b	Mn	Cl	GlyGly	-$CH_2CONHCH_2$-
3c	Re	Br	GlyGly	-$CH_2CONHCH_2$-
4a	Mn	Br	GlyVal	-$CH_2CONHCH(^iPr)$-
4c	Re	Br	GlyVal	-$CH_2CONHCH(^iPr)$-
5a	Mn	Br	GlyGlyGly	-$CH_2CONHCH_2CONHCH_2$-
5c	Re	Br	GlyGlyGly	-$CH_2CONHCH_2CONHCH_2$-

1a M = Mn, X = Br
1b M = Mn, X = Cl
1c M = Re, X = Br

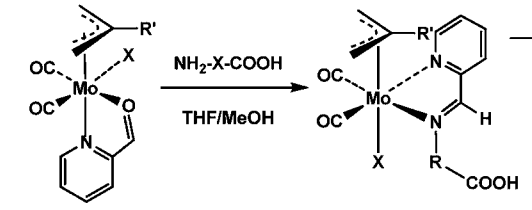

	X	R'	Péptide	R
3d	Cl	Me	GlyGly	-$CH_2CONHCH_2$-
3e	Br	Me	GlyGly	-$CH_2CONHCH_2$-
3f	Br	H	GlyGly	-$CH_2CONHCH_2$-
4d	Cl	Me	GlyVal	-$CH_2CONHCH(^iPr)$-
4e	Br	Me	GlyVal	-$CH_2CONHCH(^iPr)$-
5d	Cl	Me	GlyGlyGly	-$CH_2CONHCH_2CONHCH_2$-

1d X = Cl, R'= Me
1e X = Br, R'= H
1f X = Br, R'= Me

Scheme 4. Effect on the Acidity of the Hydrogens of Ca of Pyridoxal-5′-phosphate (Top) and Comparison with the Effect of Coordination of the Iminopyridine Ligands to Rhenium (Bottom)

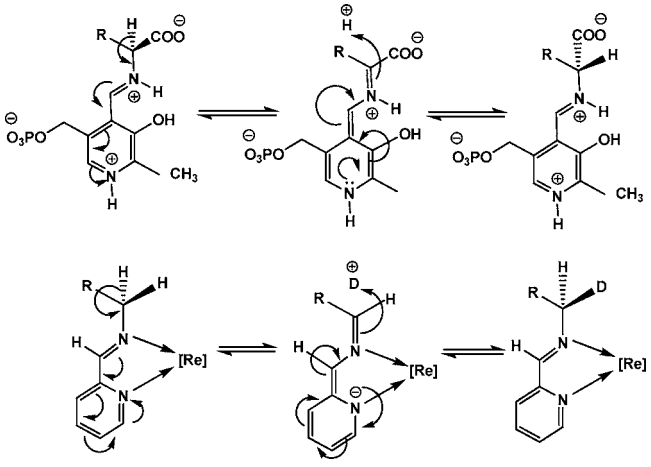

In contrast, in the solid state structure of the molybdenum methylserine derivative **2d**, two independent molecules were found in the asymmetric unit. Noticeably, each molecule is associated to its enantiomer through concerted hydrogen bonds involving O−H···Cl, thus forming two independent series of dimers consisting of $\mathbf{R_2^2(14)}$ rings (Figure 2).

The presence of additional NH, C═O, and COOH groups in the peptide derivatives **3** (Gly-Gly), **4** (Gly-Val), and **5** (Gly-Gly-Gly) gives rise to more complex arrangements. Thus, for manganese and rhenium complexes derived from glycylglycine, **3a−c**, there are infinite chains **C(4)** of antiparallel molecules (Figures 3 and 4, for **3b** see Supporting Information, Figure S1) linked through hydrogen bonds involving the peptidic N−H···O atoms. The terminal carboxylic OH group is bonded (**D**) to a solvent molecule of THF (in **3a**) or acetone (in **3c**). Interestingly, **3a** and **3c** differ only in the conformation of the peptide chain, which is extended in **3a** but bent in the Re complex **3c**. For **3b**, analogous to **3a** but with Cl instead of Br, the conformation is similar to that of the Re complex **3c** (see Supporting Information, Figure S1).

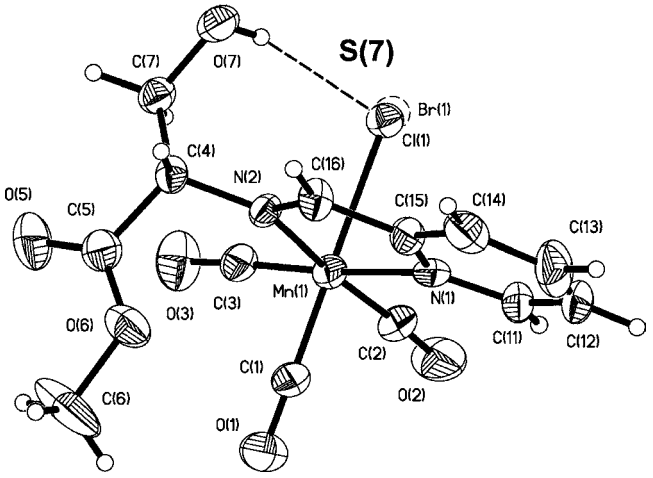

Figure 1. Perspective view of compound **2a** (major isomer, $R_{Mn}S_C$) showing the atom numbering. There is Cl/Br disorder with partial occupancy of 0.594 for Cl(1) and 0.406 for Br(1). Selected bond lengths (Å) and angles (deg): Mn(1)−C(1) 1.702(13), Mn(1)−C(2) 1.765(13), Mn(1)−C(3) 1.728(13), Mn(1)−Br(1) 2.506, Mn(1)−Cl(1) 2.383, Mn(1)−N(1) 2.002(9), Mn(1)−N(2) 2.026(8), C(5)−O(5) 1.162(13), C(5)−O(6) 1.299(13); C(1)−Mn(1)−Br(1) 178.2(4), C(1)−Mn(1)−Cl(1) 179.6(5), C(2)−Mn(1)−N(2) 173.6(4), C(3)−Mn(1)−N(1) 175.6(4), N(2)−Mn(1)−N(1) 78.6(3), O(5)−C(5)−O(6) 125.4(13). Hydrogen bonding **S(7)**: H(7)···Br(1) 2.461, H(7)···Cl(1) 2.437; O(7)···Br(1) 3.208(7), O(7)···Cl(1) 3.177(8), O(7)−H(7)···Br(1) 167.3, O(7)−H(7)···Cl(1) 164.1.

The analogous molybdenum compound **3d**, in contrast, exhibits (peptidic) N−H···Cl intramolecular H-bonds, **S(7)**, and forms ring dimers $\mathbf{R_2^2(14)}$ through concerted (carboxylic)-O−H···O(peptidic) intermolecular H-bonds (see Figure 5).

Complex **3e**, bearing Br instead of Cl, displays a similar arrangement (see Figure S2 in the Supporting Information). However, for **3f** (Figure 6) bearing an unsubstituted allyl ligand, there are infinite chains **C(7)** involving the terminal carboxylic O—H and the internal peptidic C═O. The intramolecular **S(7)** arrangement between N—H and the halogen (Cl or Br) ligand occurs in all Mo(allyl) derivatives, although the supramolecular arrangement varies depending on

dx.doi.org/10.1021/ic2022984 | Inorg. Chem. 2012, 51, 2984−2996

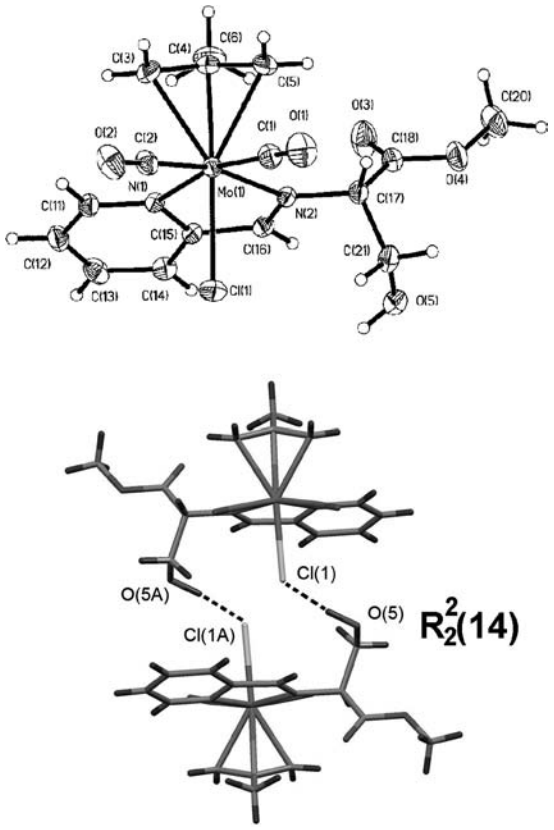

Figure 2. (Top) Thermal ellipsoid plots (30% probability) of compound **2d** (major isomer) showing the atom numbering. Selected bond lengths (Å) and angles (deg) for molecule 1: Mo(1)−C(1) 1.967(4), Mo(1)−C(2) 1.952(3), Mo(1)−C(4) 2.258(3), Mo(1)−Cl(1) 2.511(1), Mo(1)−N(1) 2.252(2), Mo(1)−N(2) 2.238(2), O(3)−C(18) 1.194(4), O(4)−C(18) 1.317(4); C(1)−Mo(1)−N(1) 167.47(11), C(2)−Mo(1)−N(2) 167.12(11), C(4)−Mo(1)−Cl(1) 164.89(8), N(2)−Mo(1)−N(1) 72.90(8), O(3)−C(18)−O(4) 124.7(3). The values are similar for molecule 2. (Bottom) Mercury drawing of the arrangement of molecule 1 with its enantiomer through H-bonding, $\mathbf{R_2^2(14)}$ system: H(5A)···Cl(1) 2.424, O(5A)···Cl(1) 3.202(3), O(5A)−H(5A)···Cl(1) 140.2. The arrangement is similar for molecule 2.

the geometry of the molecule, thus being affected by the shape and conformation of the peptide side chain, and by the spatial requirements of the other ligands bonded to the metal.

Compound **4d** crystallizes enantiomerically pure in space group $P2_12_12_1$ with a Flack parameter of 0.03(4). The configuration at the metal and the Cα carbon of valine are *R* and *S*, respectively, according to the Cahn−Ingold−Prelog system[20] and its adaptation for defining chirality of these molybdenum octahedral complexes.[21] The chirality is defined by describing the chirality of a triangular face with the metal held remote from the viewer and assigning priorities to the three ligands (halogen and the two nitrogens) according to the Cahn−Ingold−Prelog system. A sample of the crystals used for the X-ray determination of **4d** were dissolved in acetone-d_6. Its ^{1}H NMR spectrum showed the presence of only one diastereoisomer, corresponding to the minor species (45%) of the reaction mixture. This, according to the X-ray determination, is assumed to be the *RS* isomer. The more soluble, major isomer (55%) could not be crystallized. It is worth noticing that the *RS* diastereoisomer undergoes partial epimerization in solution to reach an equilibrium with the *SS* (see below Spectroscopic Studies in Solution, Scheme 5).

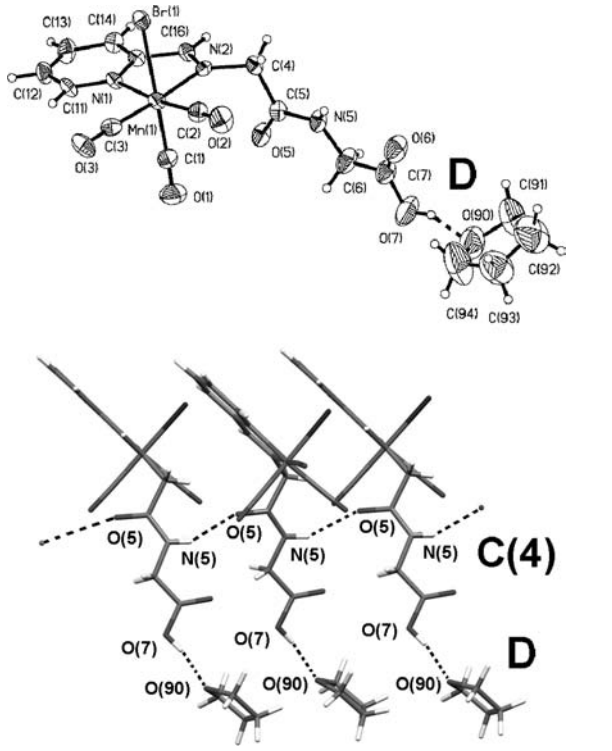

Figure 3. (Top) Perspective view of compound **3a** showing the atom numbering. Selected bond lengths (Å) and angles (deg): Mn(1)−C(1) 1.807(12), Mn(1)−C(2) 1.822(10), Mn(1)−C(3) 1.817(11), Mn(1)−Br(1) 2.547(2), Mn(1)−N(1) 2.062(6), Mn(1)−N(2) 2.035(7), C(5)−O(5) 1.221(8), C(5)−N(5) 1.313(9), C(7)−O(6) 1.182(11), C(7)−O(7) 1.317(12); C(1)−Mn(1)−Br(1) 179.4(3), C(2)−Mn(1)−N(1) 173.4(3), C(3)−Mn(1)−N(2) 174.7(3), N(2)−Mn(1)−N(1) 78.3(2), O(5)−C(5)−N(5) 122.7(8), O(6)−C(7)−O(7) 125.4(10). (Bottom) Mercury drawing displaying the hydrogen-bonding arrangement in **3a**. Selected bond lengths (Å) and angles (deg): **D** system H(7)···O(90) 1.721, O(7)···O(90) 2.611, O(7)−H(7)···O(90) 157.1; **C(4)** system H(5)···O(5) 2.131, N(5)···O(5) 3.063(8), N(5)−H(5)...O(5) 149.5.

In the solid state, the molecules of **4d** (Figure 7) exhibit a remarkable helicoidal arrangement through H-bonding involving the terminal carboxylic acid hydroxyl O(4)−H(4) to the peptidic oxygen O(3) of an adjacent molecule related to the former by a 2-fold screw axis. Therefore, this arrangement propagates along the 2_1 axis, completing a turn of the helix every two molecules. Figure 7 displays a side view (center) showing the relevant H-bonds and (bottom) a view of the packing along the 2_1 axis collinear with *a*. A similar arrangement is found for **4e** (see Figure S3 in the Supporting Information). The THF solvent molecule is associated to the peptidic N(3)−H(3), in contrast to other molecules presented in this work, in which the solvent THF is associated to the terminal carboxylic hydroxyl. Thus, for compound **5d**, as described for **4a**, the hydroxyl group of the terminal carboxylic acid function is hydrogen-bonded to the oxygen atom of the solvent THF.

In contrast to the arrangement in **4d**, in the structure of **5d**, the peptidic N(3)−H(3) forms an intramolecular H-bond with the chloride ligand, and the molecules are associated in dimers through concerted H-bonds involving the peptidic N(4)−H(4) and the O(3) of the complementary molecule (see Figure 8).

Spectroscopic Studies in Solution. The new iminopyridine complexes have been characterized by IR and NMR in solution. Mn and Re complexes display the band pattern expected for a *facial* tricarbonyl arrangement shifted to lower

dx.doi.org/10.1021/ic2022984 | *Inorg. Chem.* 2012, 51, 2984−2996

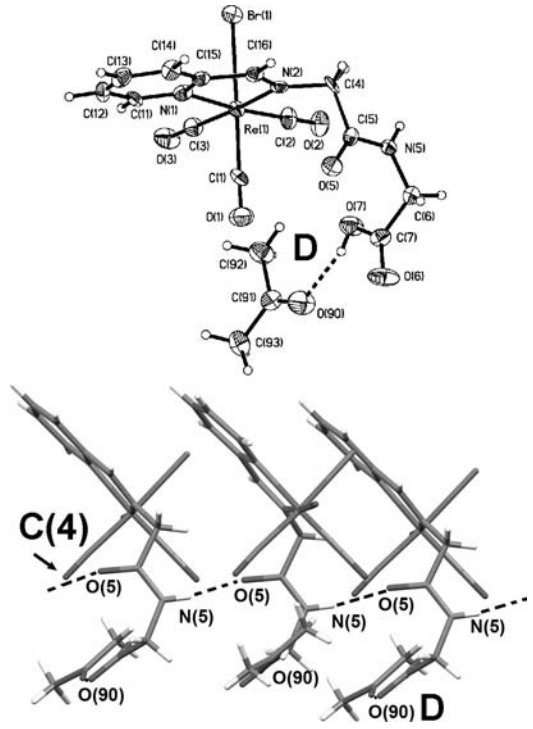

Figure 4. (Top) Perspective view of compound **3c** showing the atom numbering. Selected bond lengths (Å) and angles (deg): Re(1)−C(1) 1.933(14), Re(1)−C(2) 1.915(12), Re(1)−C(3) 1.932(9), Re(1)−Br(1) 2.623(1), Re(1)−N(1) 2.170(12), Re(1)−N(2) 2.152(8), C(5)−O(5) 1.234(11), C(5)−N(5) 1.323(12), C(7)−O(6) 1.187(13), C(7)−O(7) 1.328(14); C(1)−Re(1)−Br(1) 174.6(4), C(2)−Re(1)−N(1) 174.0(4), C(3)−Re(1)−N(2) 174.7(7), N(2)−Mn(1)−N(1) 75.3(4), O(5)−C(5)−N(5) 123.0(9), O(6)−C(7)−O(7) 124.9(12). (Bottom) Mercury drawing displaying the hydrogen-bonding arrangement in **3c**. Selected bond lengths (Å) and angles (deg): **D** system H(7)···O(90) 1.766, O(7)···O(90) 2.678(13), O(7)−H(7)···O(90) 163.2; **C(4)** system H(5)···O(5) 1.810, N(5)···O(5) 2.827(10), N(5)−H(5)···O(5) 169.0.

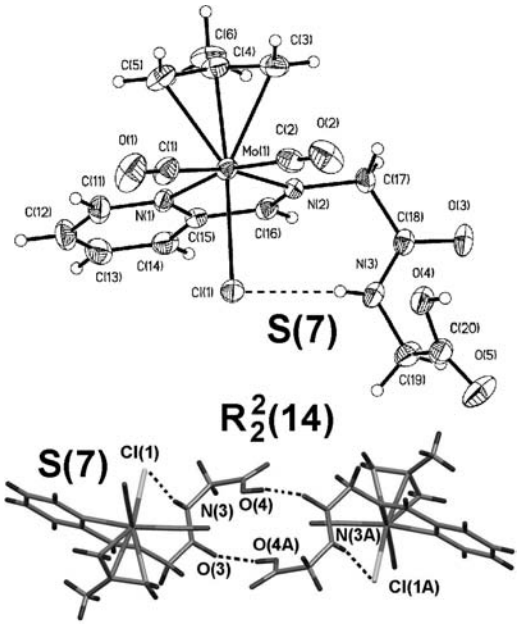

Figure 5. (Top) Perspective view of compound **3d** showing the atom numbering. Selected bond lengths (Å) and angles (deg): Mo(1)−C(1) 1.958(4), Mo(1)−C(2) 1.967(4), Mo(1)−C(4) 2.244(3), Mo(1)−Cl(1) 2.509(1), Mo(1)−N(1) 2.241(2), Mo(1)−N(2) 2.243(2), O(3)−C(18) 1.240(3), N(3)−C(18) 1.315(4), O(5)−C(20) 1.196(4), O(4)−C(20) 1.315(4); C(1)−Mo(1)−N(2) 168.45(12), C(2)−Mo(1)−N(1) 167.62(11), C(4)−Mo(1)−Cl(1) 164.30(9), N(1)−Mo(1)−N(2) 73.23(8), O(3)−C(18)−N(3) 123.4(3), O(5)−C(20)−O(4) 124.4(3). (Bottom) Mercury drawing displaying the hydrogen-bonding arrangement in **3d**, **S(7)** system: H(3)···Cl(1) 2.280, N(3)···Cl(1) 3.198(1), N(3)−H(3)···Cl(1) 147.59. In $\mathbf{R_2^2(14)}$ system: H(4)···O(3) 1.708, O(4)···O(3) 2.632(1), O(4)−H(4)···O(3) 167.61.

frequencies than those of the parent pyca complexes **1a−c**. In the case of the molybdenum complexes, the reaction involves the reorganization of the ligands (see Schemes 2 and 3), and the two bands corresponding to the *cis*-dicarbonyl grouping are shifted to higher frequencies (about 15 cm^{-1}) from those of the parent compounds **1d−f**, as we had observed previously.[13] In all cases the progress of the reactions can be easily monitored by IR spectroscopy in solution.

The ^1H NMR spectra of all new complexes show the expected characteristic five signals corresponding to the five protons of the iminopyridine fragment in the region δ 10−7 ppm, and the signals of the protons of the amino ester or peptide side chain.

The peptide derivatives **3−5** display broad signals corresponding to the carboxylic O*H* around δ 11 ppm, and to the amide N*H* around δ 8 ppm. Two-dimensional homonuclear gradient COSY and NOESY and heteronuclear gradient correlation HSQC experiments have been used to assign the signals. A detailed description of these NMR experiments is given in the Supporting Information.

The rhenium compounds are stable in solution of acetone-d_6 for a long time (at least 4−6 weeks). Successive ^1H NMR spectra showed that the protons of the carboxylic COO*H* and amido CON*H* groups interchanged deuterium with the solvent, as could be expected. Interestingly, after a long time (10 days at room temperature) the CH_2 protons in *alpha* position from the imino nitrogen of the peptide were also involved in H/D *exchange* (see Figures S12−S14 in the Supporting Information). Moreover, the H/D exchange does not affect the C*H* or CH_2 intercalated between the peptidic bonds. This is consistent with the absence of racemization in the crystal structure of the complex derived from GlyVal (**4d**). The acidity of these hydrogen atoms at C^α adjacent to iminopyridine is relevant in the mechanism of enzyme catalyzed reactions (see Scheme 4). It is well established that the formation of adducts between α-amino acids and coenzyme PLP (pyridoxal-5′-phosphate) gives a place to a notable increase in the acidity of the hydrogens of the C^α which accounts for their reactivity in a number of reactions such as the enzymatic racemization of the L-alanine, transaminations, decarboxylations, etc.[22] The iminopyridine complexes derived from amino acids undergo reactions similar to those catalyzed by the coenzyme PLP. Therefore, the H/D exchange can be rationalized as shown in Scheme 4, which also shows the similarity with the coenzyme PLP which joins the amino acid by forming an iminic link with the NH_2 group.

It has been pointed out above that complex **4d** derived from Gly-L-Val undergoes epimerization in solution. A sample of enantiopure crystals **4d** (minor, *RS*) was dissolved in acetone-d_6, and the epimerization process was monitored by ^1H NMR. The equilibrium (ratio *RS*/*SS* 45/55, same as found in the reaction mixture) was reached after 14 days at room temperature.

The observations (see Supporting Information Figure S10) are consistent with an inversion at the metal while the configuration of C_α of the Val residue is maintained. Since the well-known trigonal-twist[21] mechanism affecting the allyldicarbonyl fragment does not account for the inversion at the metal,

dx.doi.org/10.1021/ic2022984 | *Inorg. Chem.* 2012, 51, 2984−2996

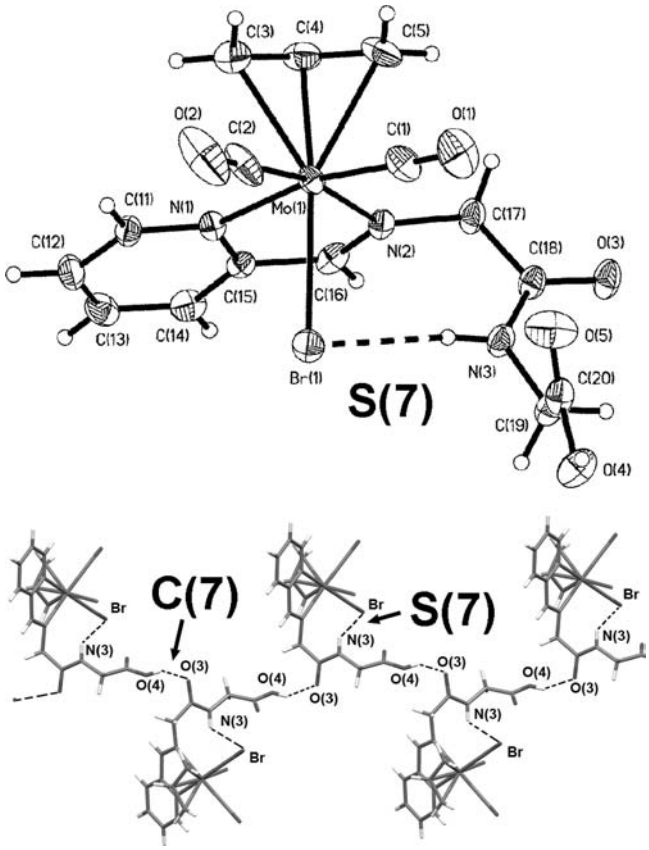

Figure 6. (Top) Perspective view of compound **3f** showing the atom numbering. Selected bond lengths (Å) and angles (deg): Mo(1)−C(1) 1.954(9), Mo(1)−C(2) 1.938(10), Mo(1)−C(4) 2.190(8), Mo(1)−Br(1) 2.665(1), Mo(1)−N(1) 2.219(6), Mo(1)−N(2) 2.290(6), O(3)−C(18) 1.228(8), N(3)−C(18) 1.325(9), O(5)−C(20) 1.191(10), O(4)−C(20) 1.312(9); C(1)−Mo(1)−N(1) 168.6(3), C(2)−Mo(1)−N(2) 169.0(3), C(4)−Mo(1)−Br(1) 164.2(3), N(1)−Mo(1)−N(2) 73.2(2), O(3)−C(18)−N(3) 124.3(7), O(5)−C(20)−O(4) 124.2(8). (Bottom) Mercury drawing displaying the hydrogen-bonding arrangement in **3f**, **S(7)** system: H(3)···Br(1) 2.352, N(3)···Br(1) 3.344(6), N(3)−H(3)···Br(1) 161.3. $\mathbf{R_2^2(14)}$ system: H(4)···O(3) 1.949, O(4)···O(3) 2.792(8), O(4)−H(4)···O(3) 148.5.

some dynamic processes involving the opening and reclosing of the chelate ring of the iminopyridine must be operating in the epimerization process (Scheme 5). Some precedents for allyl molybdenum compounds have been presented.[23]

In order to evaluate the H bonding capability of the complexes in solution, DOSY (diffusion ordered spectroscopy) were carried out by using acetone-d_6 as solvent. TMS was used as the internal reference, and tributylphosphine oxide, $OPBu_3$, was used as the hydrogen acceptor[24] (a detailed description is given in the Supporting Information).

The complexes have a very low solubility in CD_2Cl_2 or $CDCl_3$ probably due to the extensive H-bonding arrangement in the solid state, as described above. It is necessary to use very polar solvents capable of breaking the intermolecular H-bonding, and consequently, the H-bonding arrangement is not maintained in solution. The results of the DOSY experiments are summarized in Table 1 which display the values of diffusion for the complexes of Re and Mo derived from peptides Gly-Gly (**3c** and **3d**), Gly-Val (**4c** and **4d**), and Gly-Gly-Gly (**5c** and **5d**) in the absence of $OPBu_3$. The values are given in the first column as the ratio D/D_{TMS} where TMS is used as internal reference for consistency (see Supporting Information for details).

When a good acceptor for H-bonding, such as $OPBu_3$, is added to the sample, it interacts with the protons of NH(amide) and COOH. Figure 9 shows successive spectra for the derivative **5c**. It can be clearly observed that the amide protons are shifted to lower fields on addition of increasing amounts of $OPBu_3$.[25] It is interesting to notice that the shift is bigger for the amide proton labeled as NH(a) than for NH(b). This can be attributed to the electron withdrawing ability of the imine group bonded to the metal. Thus, the imine group CONH(a), closer to the imine, is a better H-donor than CONH(b). For compound **5c** (Figure 9), in the spectrum corresponding to the addition 3.0 equiv of $OPBu_3$, the shifts are 0.42 ppm for NH(a) and only 0.1 ppm for NH(b).

The interaction of $OPBu_3$ with the peptide side chains of the iminopyridine reduces the diffusion of the resulting H-bonded complex, as can be observed in the values of the second column of Table 1. As an example, Figure 10 shows the DOSY spectra of derivative **3c** (Re, Gly-Gly) in the absence of and in the presence of 2 equiv of $OPBu_3$. Following the method of Cabrita and Berger[26] it is possible to evaluate the hydrodynamic radii of the species from the measured diffusion values (D/D_{TMS}). The results are collected in Table 1 (third column). The biggest increases in hydrodynamic radii are observed for the Gly-Gly-Gly derivatives (11% for **5c**, 16% for **5d**) which contain three H-bond donors, while derivatives of Gly-Gly or Gly-Val have only two possible H-donors. In all cases, the increase of hydrodynamic radii is bigger for Mo complexes than for the Re derivatives. This may be due to the fact that, in the absence of $OPBu_3$, the molybdenum compounds are more folded than those of Re due to the presence of intramolecular H-bonds of type **S(7)** in the Mo compounds (see above).

CONCLUSION

Complexes bearing pyridine-2-carboxaledehyde (pyca) ligand as κ^2-(N,O) chelate are excellent precursors to obtain iminopyridine

Scheme 5. Interconversion of the *RS* and *SS* Isomers of Compound 4d

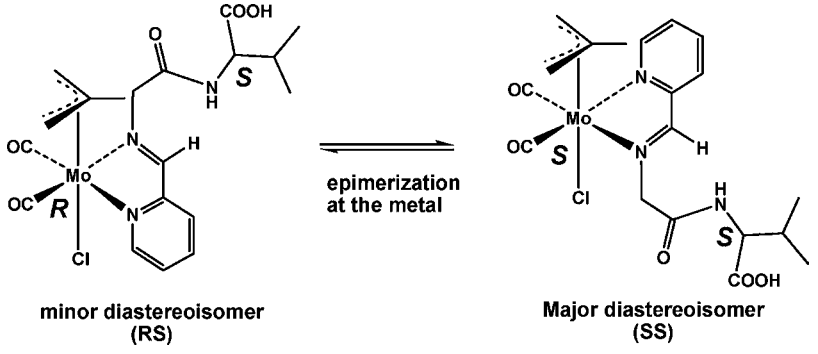

dx.doi.org/10.1021/ic2022984 | Inorg. Chem. 2012, 51, 2984−2996

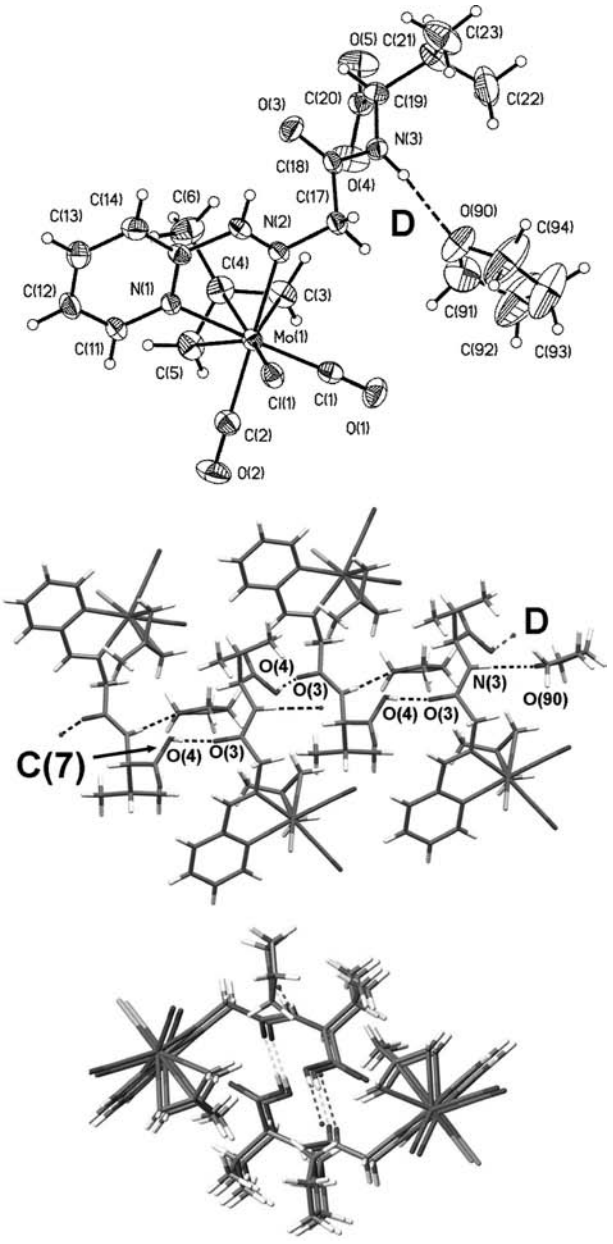

Figure 7. (Top) Perspective view of compound **4d** (minor isomer $R_{Mo}S_C$). The letters refer to the configuration at the metal and the C^{α} of valine, respectively, showing the atom numbering. Selected bond lengths (Å) and angles (deg): Mo(1)−C(1) 1.970(4), Mo(1)−C(2) 1.958(4), Mo(1)−C(4) 2.241(3), Mo(1)−Cl(1) 2.493(1), Mo(1)−N(1) 2.240(3), Mo(1)−N(2) 2.247(3), O(3)−C(18) 1.215(4), N(3)−C(18) 1.316(4), O(5)−C(20) 1.185(4), O(4)−C(20) 1.289(4). (Center) Mercury drawing showing the helicoidal arrangement of molecules through H-bonding in the solid state, **D** system: H(3)···O(90) 1.891, N(3A)···O(90) 2.881(4), N(3A)−H(3A)···O(90) 160. **C(7)** system: H(4)···O(3) 1.688, O(4)···O(3) 2.624(4), O(4)−H(4)···O(3A) 175.6. (Bottom) Mercury drawing of the molecular packing in the direction of propagation of the helices.

complexes derived from L-methylserine, the dipeptides Gly-Gly and Gly-L-Val and from the tripeptide Gly-Gly-Gly. All compounds are obtained in high isolated yields, after facile purification procedures. In the derivatives of the chiral methylserine amino ester, the acidity of the hydrogen in Cα produces partial or complete racemization at the α-carbon, while no racemization is observed for the dipeptide Gly-L-Val derivatives.

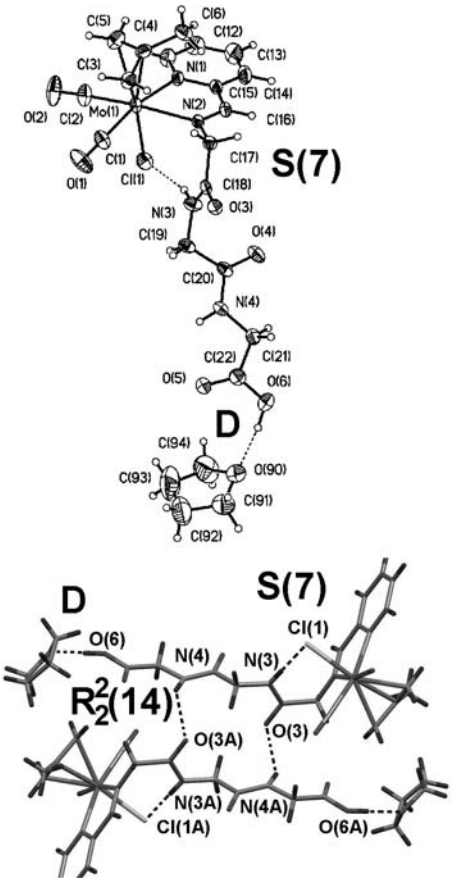

Figure 8. (Top) Perspective view of compound **5d** showing the atom numbering. Selected bond lengths (Å) and angles (deg): Mo(1)−C(1) 1.949(6), Mo(1)−C(2) 1.962(6), Mo(1)−C(4) 2.243(6), Mo(1)−Cl(1) 2.488(2), Mo(1)−N(1) 2.223(4), Mo(1)−N(2) 2.275(4), C(18)−O(3) 1.233(6), C(18)−N(3) 1.322(7), C(20)−O(4) 1.221(6), C(20)−N(4) 1.332(7), C(22)−O(5) 1.196(7), C(22)−O(6) 1.318(8); C(1)−Mo(1)−N(1) 166.5(2), C(2)−Mo(1)−N(2) 169.6(2), C(4)−Mo(1)−Cl(1) 165.8(1), N(1)−Mo(1)−N(2) 73.08(15), O(3)−C(18)−N(3) 122.2(5), O(4)−C(20)−N(4) 122.4(5), O(5)−C(22)−O(6) 124.4(6). (Bottom) Mercury drawing displaying the hydrogen-bonding arrangement in **3f**, **S(7)** system: H(3)···Cl(1) 2.179, N(3)···Cl(1) 3.181(6), N(3)−H(3)···Cl(1) 163.5. $\mathbf{R_2^2(14)}$ system: H(4)···O(3) 2.431, N(4)···O(3) 3.130(6), N(4)−H(4)···O(3) 136.1. **D** system: H(6)···O(90) 1.77, O(6)···O(90) 2.699(8), O(6)−H(6)···O(90) 171.

Table 1. Diffusion Coefficients in Acetone-d_6 Referred to TMS of Complexes 3c−5c and 3d−5d as Extracted from the ^{1}H-DOSY Plots and Changes in Hydrodynamic Radii after Addition of $OPBu_3$

compd	without $OPBu_3$ D/D_{TMS}	with $OPBu_3$ D/D_{TMS}	Δr
Rhenium Complexes			
3c (Re, Gly-Gly)	0.39	0.35	1.11
4c (Re, Gly-Val)	0.44	0.41	1.08
5c (Re, Gly-Gly-Gly)	0.36	0.31	1.15
Molybdenum Complexes			
3d (Mo, Gly-Gly)	0.42	0.36	1.16
4d (Mo, Gly-Val)	0.36	0.32	1.12
5d (Mo, Gly-Gly-Gly)	0.35	0.28	1.26

Methylserine derivatives and those containing dipeptides and tripeptide show interesting patterns of hydrogen bonding in the solid state. These patterns depend markedly on the geometry of the molecules, and the number and polarity of N−H and O−H

dx.doi.org/10.1021/ic2022984 | Inorg. Chem. 2012, 51, 2984−2996

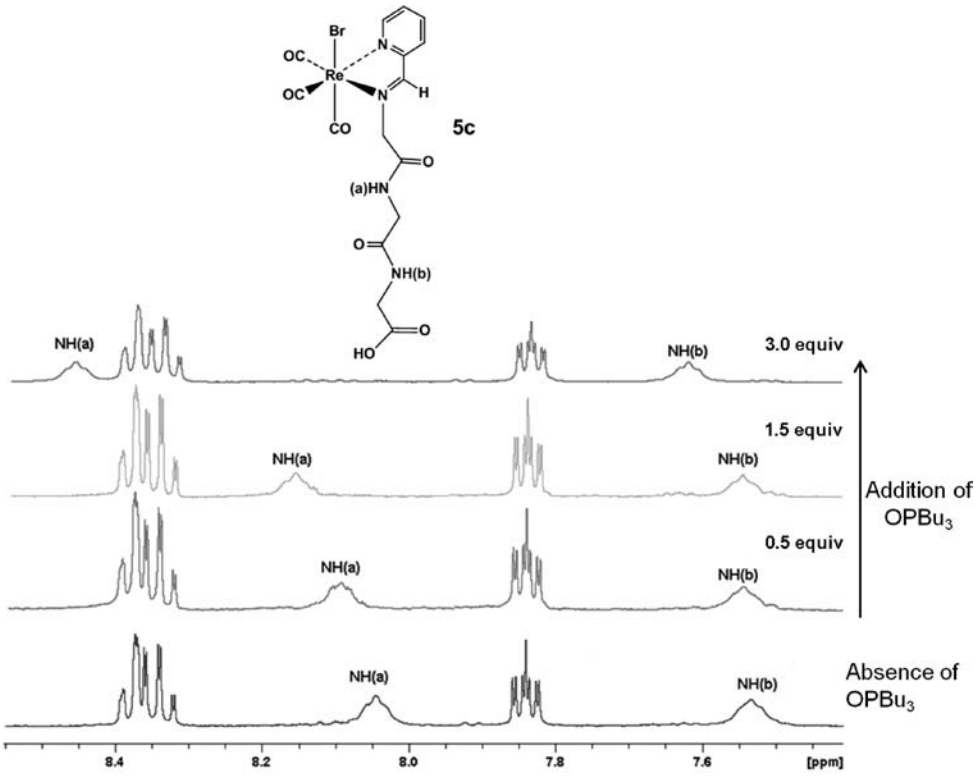

Figure 9. ^{1}H NMR spectra in acetone-d_6 showing the low-field shift of the NH protons on addition of $OPBu_3$.

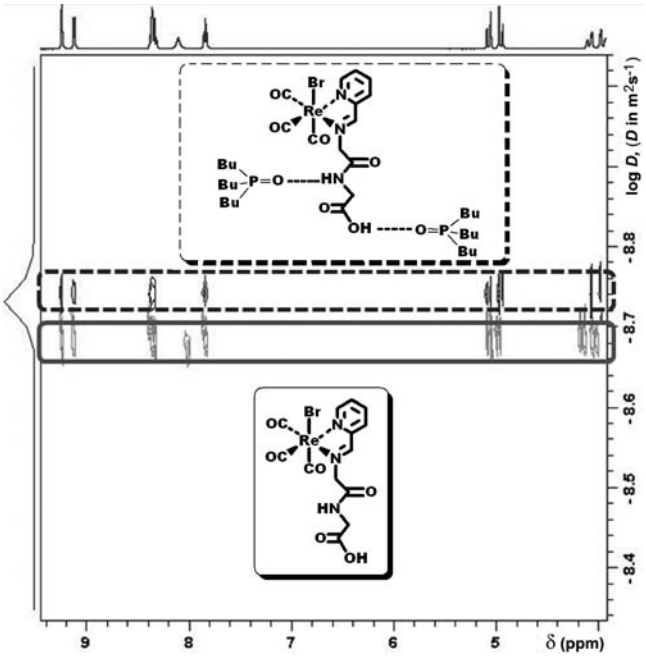

Figure 10. DOSY spectra in acetone-d_6 of the Re derivative of GlyGly (**3c**) without (—) and with (---) $OPBu_3$.

groups available, as well as the presence of solvent molecules, such as THF or acetone, capable of acting as H-bonding acceptors through the oxygen atom.

The usual head-to-head arrangement usually found[9a] for simpler carboxylic acids is not found when there are additional C═O, N—H, or O—H functions capable of H-bonding. In many cases, the terminal carboxylic O−H function is engaged in a "terminal" H-bond with a polar molecule of solvent (THF or acetone). In such cases, there is an infinite chain of H-bonding involving internal N—H and C═O functions. For the longer tripeptide Gly-Gly-Gly a discrete, dimeric association is observed, in which the peptide chains show an antiparallel arrangement, with a complementary disposition of the internal N—H and C═O functions. The H-bonding interaction of the peptide hydrogens has been studied by DOSY experiments in solution, showing a significant increase in the hydrodynamic radii of the compounds upon addition of $OPBu_3$.

■ EXPERIMENTAL SECTION

Materials and General Methods. All operations were performed under an atmosphere of dry nitrogen using Schlenk and vacuum techniques. Dichloromethane and acetonitrile were distilled from CaH_2. THF and diethylether were distilled from Na/benzophenone. Hexane was distilled from Na. Literature procedures for the preparation of starting materials are quoted in each case. Ligands and other reagents were purchased and used without purification unless otherwise stated. Silicagel 60 (230−400 mesh ASTM, Merck) was used for chromatography. Kieselguhr (diatomaceous earth, Merck) was used for filtration. IR spectra in solution were recorded with a Perkin-Elmer Spectrum RX I FT-IR instrument, using cells with CaF_2 windows. All NMR solvents were stored over molecular sieves and degassed prior to use. NMR experiments were measured on a Bruker AV-400 spectrometer. Chemical shift values are given in ppm (Scheme 6). ^{1}H and ^{13}C chemical shifts are referenced to TMS.

Complexes **1a−d** were synthesized as reported previously.[12] New complexes **1e** and **1f** were prepared in a similar way (see Supporting Information).

fac-[MnBr(CO)$_3$(py-2-C(H)═NCH(CH$_2$OH)COOCH$_3$] (***2a***). To a solution of $[H_3NCH(CH_2OH)COOCH_3]Cl$ (0.096 g, 0.61 mmol) and NEt_3 (0.062 g, 0.61 mmol) in ethanol (25 mL) was added compound **1a** (0.200 g, 0.614 mmol), and the mixture was refluxed for 15 min. The solvent was evaporated *in vacuo*, and the residue was taken up in CH_2Cl_2 and chromatographed on silica gel. Elution with THF gave **2a** as a red zone. The red band was collected, dried with magnesium sulfate, and filtered through kieselguhr. Addition of hexane and slow evaporation

dx.doi.org/10.1021/ic2022984 | Inorg. Chem. 2012, 51, 2984−2996

Scheme 6. Atom Labeling Scheme Used in the NMR Studies for the Iminopyridine and Allyl Ligands

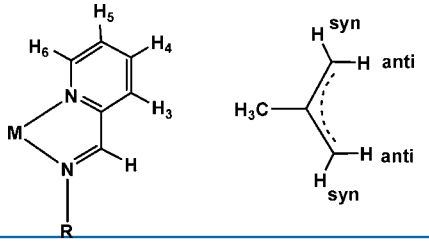

at reduced pressure gave compounds **2a** as red microcrystals. Yield 0.190 g, 72%. Anal. Calcd for $C_{13}H_{12}BrMnN_2O_6$: C 36.56, H 2.83, N 6.56. Found C 36.65, H 2.75, N 6.97. IR (CH_2Cl_2): ν(CO) 2033 vs, 1939 s(br), 1744 m (ester), cm^{-1}. IR (THF): ν(CO) 2029 vs, 1936 s, 1929 s, 1744 m (ester), cm^{-1}. ^1H NMR (acetone-d_6): isomer ratio M(ajor)/m(inor) = 80/20 δ = 9.33 (M) [d(5), 1H, pyH^6], 9.28 (m) [d(5), 1H, pyH^6], 9.00 (m) [s, 1H, py-C(*H*)=N], 8.94 (M) [s, 1H, py-C(*H*)=N], 8.31 (M + m) [m(br), 2H, pyH^3 pyH^4], 7.86(M) [m, 1H, pyH^5], 7.80 (m) [m, 1H, pyH^5], 5.25 (m) [m, 1H, NCHCOO], 5.01(M) [m(br), 1H, NCHCOO], 4.54 (M + m) [m, 1H, CH_2OH], 4.11 (M + m) [m(br), 1H, CH_2OH], 3.50 (M + m) [br, 1H, OH], 3.82 (M + m) [br, 3H, OCH_3] ppm.

*[MoCl(η3-methallyl)(CO)$_2$(py-2-C(H)=NCH(CH$_2$OH) COOCH$_3$)] (**2d**).* Compound **1d** (0.100 g, 0.286 mmol), [H_3NCH(CH_2OH)-$COOCH_3$]Cl (0.045 g, 0.29 mmol), and K_2CO_3 (0.118 g, 0.858 mmol) were refluxed in THF (25 mL) for 90 min The solvent was evaporated *in vacuo*, and the residue was dissolved in CH_2Cl_2 and filtered through kieselguhr. Addition of hexane and slow evaporation at reduced pressure gave compound **3c** as brown microcrystals. Yield 0.084 g, 65%. Anal. Calcd for $C_{16}H_{19}ClMoN_2O_5$: C 42.64, H 4.25, N 6.22. Found: C 42.56, H 4.36, N 6.49. IR (CH_2Cl_2): ν(CO) 1956 vs, 1874 s, 1744 m (ester), cm^{-1}. ^1H NMR ($CDCl_3$): isomer ratio M(ajor)/m(inor) = 80/20. δ = 8.80−8.71 (M + m) [m, 2H, py-C(*H*)=N, pyH^6], 7.98 (M + m) [m, 1H, pyH^4], 7.84(M + m) [m, 1H, pyH^3], 7.53(M) and 7.57(m) [m 1H, py H^5], 5.00 (M + m) [m, 1H, NCHCOO], 4.36 (M + m) [m, 1H, CH_2OH], 4.24 (M + m) [m, 1H, CH_2OH], 3.89 (m) and 3.86 (M) [s, 3H, OCH_3], 3.10 (M + m) [a, 1H, OH], 2.84 (M + m) [d(3), 1H H^{syn}], 2.79 (M + m) [d(3), 1H, H^{syn}], 1.44 (M + m) [m, 1H, H^{anti}], 1.38−1.37 (M + m) [m, 4H H^{anti}, CH_3(allyl)] ppm. ^1H NMR (acetone-d_6): isomer ratio M(ajor)/m(inor) = 80/20. δ = 8.95 (m) and 8.90 (M) [s, 1H, py-C(*H*)=N], 8.85(m) and 8.80 (M) [d(5), 1H, pyH^6], 8.20 (M + m) [m, 2H, pyH^3, pyH^4], 7.73 (M + m) [m, 1H, pyH^5], 5.07 (M + m) [m, 1H, NC*H*], 4.17 (M + m) [m, 2H, CH_2OH], 3.83 (M) and 3.80 (m) [s, 3H, OCH_3], 2.92 (M + m) [a, 1H, OH], 2.89 (M + m) [d(3), 1H H^{syn}], 2.86 (M + m) [d(3), 1H, H^{syn}], 1.37 (M + m) [m, 3H, CH_3(allyl)], 1.26 (M + m) [m, 1H, H^{anti}], 1.22 (M + m) [m, 1H, H^{anti}] ppm.

*fac-[MnBr(CO)$_3$(py-2-C(H)=NCH$_2$CONHCH$_2$COOH)] (**3a**).* Compound **1a** (0.200 g, 0.614 mmol) and glycylglycine (0.081 g, 0.61 mmol) were refluxed in EtOH (25 mL) overnight. The solvents were evaporated in vacuo, and the residue was washed with 1:1 CH_2Cl_2/hexane (2 × 10 mL). The resulting solid residue was dissolved in THF and filtered through kieselguhr. Slow diffusion of hexane into a solution of **3a** in THF at −20 °C afforded red crystals, one of which was used for X-ray diffraction. Yield 0.259 g, 82%. Anal. Calcd for $C_{13}H_{11}BrMnN_3O_6$·THF: C 39.86, H 3.74, N 8.20. Found: C 39.57, H 3.96, N 8.39. IR (CH_2Cl_2): ν(CO) 2032 vs, 1937 vs (br), cm^{-1}. IR (THF): ν(CO) 2025 vs, 1929 vs (br), 1738 m (acid), 1690 m (amide) cm^{-1}. ^1H NMR (acetone-d_6): δ = 9.27 [d(4), 1H, pyH^6], 8.84 [s, 1H, py-C(*H*)=N], 8.24−8.18 [m, 2H, pyH^3, pyH^4], 8.09 [br, 1H, CON*H*], 7.77 [m, 1H, pyH^5], 5.16 [d(12), 1H, NCH_2CONH], 4.90 [d(12), 1H, NCH_2CONH], 4.13 [m(br), 2H, CH_2COOH] ppm.

*fac-[MnCl(CO)$_3$(py-2-C(H)=NCH$_2$CONHCH$_2$COOH)] (**3b**).* Compound **3b** was prepared as described above for compound **3a**, starting from compound **1b** (0.200 g, 0.710 mmol) and glycylglycine (0.094 g, 0.71 mmol) in ethanol (25 mL). The workup was as described for **2a** to afford compound **2b**. Slow diffusion of hexane into a solution of **3b** in THF at −20 °C afforded red crystals, one of which was used for X-ray diffraction. Yield 0.271 g, 82%. Anal. Calcd for $C_{13}H_{11}$-$ClMnN_3O_6$·THF: C 43.65, H 4.09, N 8.98. Found: C 43.70, H 3.99, N 8.75. IR (THF): ν(CO) 2028 vs, 1930 vs (br), 1738 m (acid), 1690 m (amide), cm^{-1}. ^1H NMR (acetone-d_6): δ = 9.26 [br, 1H, pyH^6], 8.91 [br, 1H, py-C(*H*)=N], 8.31−8.17 [m(br), 2H, pyH^3, pyH^4], 8.09 [br, 1H, N*H*CO], 7.80 [a, 1H, pyH^5], 5.11 [br, 1H, NCH_2], 4.93 [br, 1H, NCH_2], 4.19 [br, 2H, CH_2COOH] ppm.

*fac-[ReBr(CO)$_3$(py-2-C(H)=NCH$_2$CONHCH$_2$COOH)] (**3c**).* Compound **1d** (0.150 g, 0.328 mmol) and glycylglycine (0.043 g, 0.33 mmol) were refluxed in EtOH (25 mL) for 2 h. The solvents were evaporated in vacuo, and the residue was washed with hexane (2 × 15 mL). The resulting solid residue was dissolved in THF and filtered through kieselguhr. Addition of hexane and slow evaporation at reduced pressure gave compound **3d** as red microcrystals. Yield 0.168 g, 80%. Anal. Calcd for $C_{13}H_{11}BrN_3O_6Re$·THF: C 31.73, H 2.98, N 6.53. Found: C 31.50, H 2.67, N 6.35. IR (THF), ν(CO): 2022 vs, 1920 s, 1907 s, 1746 m (acid), 1696 m (amide), cm^{-1}. ^1H NMR (acetone-d_6): δ = 11.08 [br, 1H, COO*H*], 9.23 [s, 1H, py-C(*H*)=N], 9.11 [d(5), 1H, pyH^6], 8.37−8.31 [m, 2H, pyH^3, pyH^4], 8.01 [br, 1H, CON*H*], 7.82 [m, 1H, pyH^3], 5.05 [d(14), 1H, NCH_2], 4.97 [d(14),1H, NCH_2], 4.14 [dd(18, 6), 1H, CH_2COOH], 4.02 [dd(18, 6), 1H, CH_2COOH] ppm.

*[MoCl(η^3-methallyl)(CO)$_2$(py-2-C(H)=NCH$_2$CONH−CH$_2$COOH)] (**3d**).* Compound **1d** (0.200 g, 0.572 mmol) and glycylglycine (0.076 g, 0.57 mmol) were refluxed in THF (25 mL) and MeOH (5 mL) for 4 h. The solvents were evaporated in vacuo, and the residue was washed with hexane and Et_2O. The resulting solid residue was dissolved in THF and filtered through kieselguhr. Addition of hexane and slow evaporation at reduced pressure gave compound **3d** as dark brown microcrystals. Yield 0.225 g, 85%. Anal. Calcd for $C_{16}H_{18}ClMoN_3O_5$: C 41.44, H 3.91, N 9.06. Found: C 41.38, H 4.00, N 8.98. IR (THF): ν(CO): 1951 vs, 1874 s, 1750 m (acid), 1687 (amide), cm^{-1}. ^1H NMR (acetone-d_6) δ = 11.10 [br, 1H, COO*H*], 8.83 [d(5), 1H, pyH^6], 8.80 [s, 1H, py-C(*H*)=N], 8.20 [td(8, 2), 1H, pyH^4], 8.15 [m, 1H, pyH^3], 8.12 [m(br), 1H, N*H*CO], 7.73 [m 1H, pyH^5], 4.78 [d(15), 1H, NCH_2], 4.65 [d(15), 1H, NCH_2], 4.12 [dd(18, 6), 1H, CH_2COOH], 3.95 [dd(18, 6), 1H, CH_2COOH], 3.03 [dd(4, 1), 1H, H^{syn}], 2.87 [dd(4, 1), 1H, H^{syn}], 1.37 [s, 3H, CH_3(allyl)], 1.25 [s, 1H, H^{anti}], 1.14 [s, 1H, H^{anti}] ppm.

*[MoBr(η^3-methallyl)(CO)$_2$(py-2-C(H)=NCH$_2$CONH−CH$_2$COOH)] (**3e**).* Compound **3e** was prepared as described above for compound **3d**, starting from compound **1e** (0.200 g, 0.508 mmol) and glycylglycine (0.067 g, 0.51 mmol) in THF (25 mL) and MeOH (5 mL). The workup was as described for **3d** to afford compound **3e**. Yield 0.224 g, 80%. Anal. Calcd for $C_{16}H_{18}BrMoN_3O_5$: C 37.82, H 3.57, N 8.27. Found: C 37.91, H 3.69, N 8.21. IR (THF): ν(CO) 1951 vs, 1875 s, 1745 m (acid), 1687 (amide), cm^{-1}. ^1H NMR (acetone-d_6) δ = 11.23 [br, 1H, COO*H*], 8.80 [d(5), 1H, pyH^6], 8.72 [s, 1H, py-C(*H*)=N], 8.18−8.14 [m, 2H, pyH^3, pyH^4], 8.10 [br 1H, N*H*CO], 7.70 [m 1H, pyH^5], 4.81 [d(15), 1H, NCH_2], 4.60 [d(15), 1H, NCH_2], 4.07 [m, 2H, CH_2COOH], 3.04 [d(3), 1H, H^{syn}], 2.84 [d(3), 1H, H^{syn}], 1.29 [s, 3H, CH_3(allyl)], 1.25 [s, 1H, H^{anti}], 1.16 [s, 1H, H^{anti}].ppm.

*[MoBr(η^3-allyl)(CO)$_2$(py-2-C(H)=NCH$_2$CONH—CH$_2$COOH)] (**3f**).* Compound **3f** was prepared as described above for compound **3d**, starting from compound **1f** (0.200 g, 0.560 mmol) and glycylglycine (0.074 g, 0.56 mmol) in THF (25 mL) and MeOH (5 mL). The workup was as described for **3d** to afford compound **3f**. Yield 0.229 g, 83%. Anal. Calcd for $C_{15}H_{16}BrMoN_3O_5$: C 36.46, H 3.26, N 8.50. Found: C 36.66, H 3.14, N 8.39. IR (THF): ν(CO) 1950 vs, 1872 s, 1747 m (acid), 1687 (amide), cm^{-1}. ^1H NMR (acetone-d_6) δ = 11.25 [br, 1H, COO*H*], 8.85 [d(5), 1H, pyH^6], 8.62 [s, 1H, py-C(*H*)=N], 8.18 [m, 1H, pyH^4], 8.11 [m, 1H, pyH^3], 8.02 [br 1H, N*H*CO], 7.69 [m 1H, pyH^5], 4.78 [d(15), 1H, NCH_2], 4.62 [d(15), 1H, NCH_2], 4.08 [m, 2H, CH_2COOH], 3.33 [m, 1H, *H*(allyl)], 3.27 [m, 1H, H^{syn}], 3.14 [m, 1H, H^{syn}], 1.28 [m, 1H, H^{anti}], 1.09 [m, 1H, H^{anti}].ppm.

*fac-[MnBr(CO)$_3$(py-2-C(H)=NCH$_2$CONHCH(CH(CH$_3$)$_2$)COOH)] (**4a**).* Compound **1a** (0.200 g, 0.614 mmol) and glycyl-L-valine (0.107 g, 0.614 mmol) were refluxed in EtOH (25 mL) for 7 h. The solvents were evaporated in vacuo, and the residue was washed with hexane (2 × 15 mL). The resulting solid residue was dissolved in THF and filtered through kieselguhr. Addition of hexane and slow evaporation at reduced pressure gave compound **4a** as red microcrystals. Yield 0.233 g, 78%. Anal. Calcd for $C_{16}H_{17}BrMnN_3O_6$: C 39.86, H 3.55, N 8.71. Found: C 39.98, H 3.72, N 8.54. IR (THF): ν(CO) 2025 vs, 1930 vs (br), cm^{-1}.

dx.doi.org/10.1021/ic2022984 | *Inorg. Chem.* 2012, 51, 2984−2996

^{1}H NMR (acetone-d_6): δ = 9.25 [d(4), 1H, H^6 of py], 8.79 [s(br), 1H, py-C(H)=N], 8.22 [m(br), 2H, H^3 and H^4 of py], 7.94 [m(br), 1H, CONH], 7.76 [m(br), 1H, H^5 of py], 5.27 [m(br), 1H, NCH_2CONH], 4.86 [m(br), 1H, NCH_2CONH], 4.63 [m(br), 1H,CONHCH], 2.25 [m(br), 1H, CH(CH_3)$_2$], 1.03 [m(br), 6H, (CH_3)$_2$] ppm.

*fac-[ReBr(CO)$_3$(py-2-C(H)=NCH$_2$CONHCH(CH(CH$_3$)$_2$)COOH)] (**4c**).* Compound **1c** (0.150 g, 0.328 mmol) and glycyl-L-valine (0.057 g, 0.33 mmol) were refluxed in EtOH (25 mL) for 2 h. The solvents were evaporated in vacuo, and the residue was washed with hexane (2 × 15 mL). The resulting solid residue was dissolved in THF and filtered through kieselguhr. Addition of hexane and slow evaporation at reduced pressure gave compound **5d** as red microcrystals. Yield 0.169 g, 84%. Anal. Calcd for $C_{16}H_{17}BrN_3O_6Re$: C 31.33, H 2.79, N 6.85. Found: C 31.47, H 2.99, N 6.52. IR (THF): ν(CO) 2022 vs, 1920 s, 1908 s, cm^{-1}. ^{1}H NMR (acetone-d_6): isomer ratio M(ajor)/m(inor) = 52/48. δ = 11.10 (M + m) [br, 1H, COOH], 9.19 (m) [s, 1H, py-C(H)=N], 9.15 (M) [s, 1H, py-C(H)=N], 9.13−9.09 (M + m) [m 1H, pyH^6], 8.38−8.30 (M + m) [m, 2H, pyH^3 pyH^4], 7.92 (M) [d(8), 1H, CONH], 7.88 (m) [d(8), 1H, CONH], 7.85−7.80 (M + m) [m 1H, pyH^5], 5.20 (M) [dd(14, 1), 1H, NCH_2], 5.12 (m) [dd(14, 1), 1H, NCH_2], 5.02 (m) [dd(14, 1), 1H, NCH_2], 4.94 (M) [d(14), 1H, NCH_2], 4.58−4.52 (M + m) [m, 1H, CHCOOH], 2.34−2.22 (M + m) [m, 1H, CH(CH$_3$)$_2$], 1.08 (M) [d(7), 3H, CHCH_3], 1.04 (M) [d(7), 3H, CHCH_3], 1.01 (m) [d(7), 3H, CHCH_3], 0.98 (m) [d(7), 3H, CHCH_3] ppm.

*[MoCl(η^3-methallyl)(CO)$_2$(py-2-C(H)=NCH$_2$CONHCH(CH(CH$_3$)$_2$)-COOH)] (**4d**).* Compound **1d** (0.200 g, 0.572 mmol) and glycyl-L-valine (0.100 g, 0.572 mmol) were refluxed in THF (25 mL) and MeOH (3 mL) for 3 h. The solvents were evaporated in vacuo, and the residue was washed with hexane (2 × 15 mL). The resulting solid residue was dissolved in THF and filtered through kieselguhr. Addition of hexane and slow evaporation at reduced pressure gave both diasteroisomers of compound **4d** as brown microcrystals. Slow diffusion of hexane into a solution of **4d** in THF at −20 °C afforded black crystals of minor diasteroisomer of **4d**, one of which was used for X-ray diffraction. Yield 0.290 g, 88%. Anal. Calcd for $C_{19}H_{24}ClMoN_3O_5$·THF: C 0.47.80, H 5.58, N 7.27. Found: C 47.93, H 5.32, N 7.44. IR (THF): ν(CO) 1950 vs, 1872 s, 1734 m (acid), 1689 m, (amide), cm^{-1}. ^{1}H NMR (acetone-d_6): isomer ratio M(ajor)/m(inor) = 55/45. Isomer M(ajor) (55%) δ = 11.19 [br, 1H, COOH], 8.81 [d(5), 1H, pyH^6], 8.73 [s, 1H, pyC(H)=N], 8.20−8.12 [m, 2H, pyH^4, pyH^3], 7.99 [d(8), 1H, CONH], 7.71 [m, 1H, pyH^5], 4.88 [d(15), 1H, NCH_2], 4.59 [dd(15, 1), 1H, NCH_2], 4.44 [m, 1H, CHCOOH], 2.99 [d(4), 1H, H^{syn}], 2.86 [d(4), 1H, H^{syn}], 2.26 [m, 1H, CH(CH$_3$)$_2$], 1.33 [s, 3H, CH_3(allyl)], 1.23 [s, 1H, H^{anti}], 1.15 [s, 1H, H^{anti}], 1.04 [d(7), 3H, CHCH_3], 1.02 [d(7), 3H, CHCH_3] ppm. Isomer m(inor) (45%) δ = 11.19 [br, 1H, COOH], 8.79 [d(5), 1H, pyH^6], 8.71 [s, 1H, pyC(H)=N], 8.20−8.12 [m, 2H, pyH^4, pyH^3], 8.01 [d(8), 1H, CONH], 7.70 [m, 1H, pyH^5], 4.86 [d(15), 1H, NCH_2], 4.64 [dd(15, 1), 1H, NCH_2], 4.44 [m, 1H, CHCOOH], 2.99 [d(4), 1H, H^{syn}], 2.84 [d(4), 1H, H^{syn}], 2.26 [m, 1H, CH(CH$_3$)$_2$], 1.33 [s, 3H, CH_3(allyl)], 1.20 [s, 1H, H^{anti}], 1.12 [s, 1H, H^{anti}], 1.01 [d(7), 3H, CHCH_3], 0.99 [d(7), 3H, CHCH_3] ppm.

*[MoBr(η^3-methallyl)(CO)$_2$(py-2-C(H)=NCH$_2$CONHCH(CH(CH$_3$)$_2$)-COOH)] (**4e**).* Compound **4e** was prepared as described above for compound **4d**, starting from compound **1e** (0.200 g, 0.508 mmol) and glycylglycine (0.088 g, 0.51 mmol) in THF (25 mL) and MeOH (3 mL). The workup was as described for **4d** to afford both diasteroisomers of compound **4e**. Slow diffusion of hexane into a solution of **4e** in THF at −20 °C afforded black crystals of minor isomer of **4e**, one of which was used for X-ray diffraction. Yield 0.268 g, 85%. Anal. Calcd for $C_{19}H_{24}BrMoN_3O_5$·THF: C 0.44.39, H 5.18, N 6.75. Found: C 44.61, H 5.22, N 6.79. IR (THF): ν(CO) 1951 vs, 1874 s, 1734 m (acid), 1689 m, (amide), cm^{-1}. ^{1}H NMR (acetone-d_6): isomer ratio M(ajor)/m(inor) = 55/45. Isomer M(ajor) (55%): 11.26 [br, 1H, COOH], 8.78 [d(6), 1H, pyH^6], 8.69 [s, 1H, py-C(H)=N], 8.19−8.12 [m 1H, pyH^3, pyH^4], 8.00 [d(8), 1H, NHCO], 7.68 [m 1H, pyH^5], 4.90 [d(15), 1H, NCH_2], 4.57 [dd(15, 1), 1H, NCH_2], 4.51 [m, 1H, CHCOOH], 3.00 [d(3), 1H, H^{syn}], 2.85 [d(3), 1H, H^{syn}], 2.29 [m, 1H, CH(CH$_3$)$_2$], 1.29 [s, 3H, CH_3(allyl)], 1.24 [s, 1H, H^{anti}], 1.16[s, 1H, H^{anti}], 1.06 [d(7), 3H, CHCH_3], 1.04 [t(7), 3H, CHCH_3] ppm. Isomer m(inor) (45%): δ = 11.26 [br, 1H, COOH], 8.77 [d(6), 1H, pyH^6], 8.67 [s, 1H, py-C(H)=N], 8.17−8.14 [m 1H, pyH^3, pyH^4], 8.02 [d(8), 1H, NHCO], 7.68 [m 1H, pyH^5], 4.87 [d(15), 1H, NCH_2], 4.63 [dd(15, 1), 1H, NCH_2], 4.47 [m, 1H, CHCOOH], 3.00 [d(3), 1H, H^{syn}], 2.83 [d(3), 1H, H^{syn}], 2.27 [m, 1H, CH(CH$_3$)$_2$], 1.26 [s, 3H, CH_3(allyl)], 1.21 [s, 1H, H^{anti}], 1.14 [s, 1H, H^{anti}], 1.03 [d(7), 3H, CHCH_3], 1.01 [t(7), 3H, CHCH_3] ppm.

*fac-[MnBr(CO)$_3$(py-2-C(H)=NCH$_2$CONH−CH$_2$CONH−CH$_2$COOH)] (**5a**).* Compound **1a** (0.200 g, 0.614 mmol) and glycylglycylglycine (0.116 g, 0.614 mmol) were refluxed in EtOH (25 mL) for 9 h. The solvents were evaporated in vacuo, and the residue was washed with hexane and 1:1 CH_2Cl_2/hexane (2 × 10 mL). The resulting solid residue was dissolved inTHF/MeOH and filtered through kieselguhr. Addition of hexane and slow evaporation at reduced pressure gave compound **5a** as red-orange microcrystals.

Yield 0.255 g, 73%. Anal. Calcd for $C_{15}H_{14}BrMnN_4O_7$·THF: C 40.09, H 3.90, N 9.84. Found: C 39.97, H 3.76, N 9.45. IR (THF): ν(CO) 2025 vs, 1934 s, 1926 s, cm^{-1}.

*fac-[ReBr(CO)$_3$(py-2-C(H)=NCH$_2$CONHCH$_2$COOH)] (**5c**).* Compound **1c** (0.150 g, 0.328 mmol) and glycylglycylglycine (0.062 g, 0.33 mmol) were refluxed in EtOH (25 mL) for 2 h. The solvents were evaporated in vacuo, and the residue was washed with hexane (3 × 15 mL). The resulting solid residue was dissolved in THF and filtered through kieselguhr. Addition of hexane and slow evaporation at reduced pressure gave compound **5c** as red microcrystals.

Yield 0.172 g, 75%. Anal. Calcd for $C_{15}H_{14}BrN_4O_7Re$·THF: C 32.58, H 3.17, N 8.00. Found: C 32.72, H 3.31, N 7.89. IR (THF): ν(CO) 2022 vs, 1920 s, 1905 s, cm^{-1}. ^{1}H NMR (acetone-d_6): δ = 11.01 [br, 1H, COOH], 9.26 [s, 1H, py-C(H)=N], 9.12 [d(5), 1H, pyH^6], 8.39−8.34 [m, 2H, pyH^3, pyH^4], 8.05 [br, 1H, NCH$_2$CONH], 7.84 [m, 1H, pyH^5], 7.54 [br, 1H, CONHCH$_2$COOH], 5.06 [dd(14, 1), 1H, NCH_2CONH], 4.99 [d(14), 1H, NCH_2CONH], 4.12 [dd(17, 6), 1H, CONHCH_2CONH], 4.00−3.94 [m, 3H, CONHCH_2CONH, CH_2COOH] ppm.

*[MoCl(η^3-methallyl)(CO)$_2$(py-2-C(H)=NCH$_2$CONH−CH$_2$CONH−CH$_2$COOH)] (**5d**).* Compound **1d** (0.200 g, 0.572 mmol) and glycylglycylglycine (0.120 g, 0.634 mmol) were refluxed in THF (25 mL) and MeOH (10 mL) for 7 h. The solvents were evaporated *in vacuo*, and the residue was washed with CH_2Cl_2 (2 × 5 mL) and then extracted repeatedly with THF. The collected extracts were filtered through kieselguhr. Slow diffusion of hexane into a concentrated solution of **5d** in THF at −20 °C afforded red-orange crystals, one of which was used for X-ray diffraction. Yield 0.264 g, 78%. Anal. Calcd for $C_{18}H_{21}ClMoN_4O_6$·THF: C 0.44.57, H 4.93, N 9.45. Found: C 44.38, H 4.91, N 9.26. IR (THF): ν(CO) 1952 vs, 1874 s. ^{1}H NMR (acetone-d_6) δ = 11.06 [br, 1H, COOH], 8.84−8.81 [m, 2H, pyH^6, pyC(H)=N], 8.20−8.14 [m, 2H, pyH^3, pyH^4], 8.11 [t(br)(6), 1H, NCH$_2$CONH], 7.73 [m, 1H, pyH^5], 7.52 [t(br)(6), 1H, CONHCH$_2$COOH], 4.78 [d(15), 1H, NCH_2CONH], 4.68 [dd(15, 1), 1H, NCH_2CONH], 4.12 [dd(17, 6), 1H, CONHCH_2CONH], 3.96 [m, 2H, CH_2COOH], 3.85 [dd(17, 6), 1H, CONHCH_2CONH], 3.00 [d(4), 1H, H^{syn}], 2.87 [d(4), 1H, H^{syn}], 1.37 [s, 3H, CH_3(allyl)], 1.26 [s, 1H, H^{anti}], 1.16 [s, 1H, H^{anti}] ppm.

*X-ray Diffraction Study of **2a, 2d, 3a, 3b, 3c, 3d, 3e, 3f, 4d, 4e, and 5d**.* Crystals were grown by slow diffusion of hexane into concentrated solutions of the complexes in THF, CH_2Cl_2 (for **2d**), or acetone (for **3c**) at −20 °C. Intensity measurement was made with a Bruker AXS SMART 1000 diffractometer with graphite monochromatized Mo Kα X-radiation and a CCD area detector. Raw frame data were integrated with the SAINT[27] program. A semiempirical absorption correction was applied with the program SADABS.[28] The structures were solved by direct methods with SIR2002,[29] under WINGX,[30] and refined against F^2 with SHELXTL.[31] All non-hydrogen atoms were refined anisotropically unless otherwise stated. Hydrogen atoms were set in calculated positions and refined as riding atoms, with a common thermal parameter. In the structure of **2a** was found a disorder due to partial replacement of Br by Cl. After unsuccessful attempts to refine the halogen atoms freely, they had to be positioned at the appropriate bonding distances, and only the occupancy was refined. The final refinement gave a partial occupancy of 0.594 for Cl and 0.406 for Br. Calculations were made with SHELXTL and PARST,[32] and graphics were made with SHELXTL and MERCURY.[33] Crystal data, particular details, and CCDC reference numbers are given in Table 2.

dx.doi.org/10.1021/ic2022984 | Inorg. Chem. 2012, 51, 2984−2996

Table 2. Crystal, Measurement, and Refinement Data for the Compounds Studied by X-ray Diffraction

	2a	2d	3a	3b	3c	3d
formula	$C_{13}H_{12}Br_{0.41}Cl_{0.59}MnN_2O_6$	$C_{16}H_{19}ClMoN_2O_5{\cdot}0.5CH_2Cl_2$	$C_{13}H_{11}BrMnN_3O_6$ THF	$C_{13}H_{11}ClMnN_3O_6{\cdot}$THF	$C_{13}H_{11}BrN_3O_6ReC_3H_6O$	$C_{16}H_{18}ClMoN_3O$
M_f	400.64	493.19	512.20	467.74	629.44	463.72
cryst syst	monoclinic	triclinic	monoclinic	monoclinic	orthorhombic	triclinic
space group	$C2$	$P\bar{1}$	$P2_1/c$	$P2_1/c$	$Pna2_1$	$P\bar{1}$
a [Å]	19.772(18)	9.625(2)	23.663(3)	24.097(5)	9.562(2)	7.695(2)
b [Å]	6.835(6) Å	11.315(3)	9.677(2)	9.335(2)	9.795(3)	8.300(2)
c [Å]	11.481(10)	18.996(4)	9.539(2)	9.501(2)	21.767(6)	15.804(4)
α [deg]	90	80.184(4)	90	90	90	88.835(6)
β [deg]	98.18(3)	86.999(4)	96.507(5)	94.857(4)	90	89.667(5)
γ [deg]	90	82.720(4)	90	90	90	68.990(5)
V [Å^3]	1536(2)	2021.2(8)	2170.2(9)	2129.5(8)	2038.7(9)	942.1(4)
Z	4	4	4	4	4	2
ρ [Mg m^{-3}]	1.733	1.621	1.568	1.459	2.051	1.635
μ(Mo Kα) [mm^{-1}]	2.048	0.942	2.491	0.787	7.962	0.869
cryst size [mm^3]	0.19 × 0.08 × 0.07	0.36 × 0.12 × 0.09	0.43 × 0.26 × 0.03	0.41 × 0.25 × 0.03	0.14 × 0.07 × 0.04	0.36 × 0.17 × 0.04
F(000)	805	996	1032	960	1200	468
θ range [deg]	1.79 ≤ θ ≤ 23.29	1.09 ≤ θ ≤ 23.28	0.87 ≤ θ ≤ 23.30	0.85 ≤ θ ≤ 25.41	1.87 ≤ θ ≤ 25.37	1.29 ≤ θ ≤ 23.28
max/min transm	1/0.621 069	1/0.829 463	1/0.286 201	1/0.748 043	1/0.556 746	1/0.689 202
reflns collected	5006	13020	9416	16684	15441	4463
indep reflns [R(int)]	2201 [0.0679]	5815 [0.0283]	3117 [0.0870]	3921 [0.0398]	3736 [0.0590]	2697 [0.0177]
reflns with $I > 2\sigma(I)$	1599	4966	1948	2900	3028	2424
GOF on F^2	1.047	1.037	1.029	1.119	0.981	1.045
params/restraints	210/1	482/0	264/0	262/0	256/1	237/0
R1 (on F, $I > 2\sigma(I)$)	0.0628	0.0270	0.0625	0.0415	0.0343	0.0265
wR2 (on F^2, all data)	0.1560	0.0704	0.1742	0.1339	0.0811	0.0679
max/min $\Delta\rho$ [e Å^{-3}]	0.650/−0.409	0.383/−0.475	0.706/−0.532	0.389/−0.245	2.844/−1.108	0.379/−0.256
CCDC number	830400	830401	830402	830403	830404	830405

	3e	3f	4d	4e	5d
formula	$C_{16}H_{18}BrMoN_3O_5$	$C_{15}H_{16}BrMoN_3O_5$	$C_{19}H_{24}ClMoN_3O_5$ THF	$C_{19}H_{24}BrMoN_3O_5$ THF	$C_{18}H_{21}ClMoN_4O_6$ THF
M_f	508.18	494.16	577.91	622.37	592.88
cryst syst	triclinic	orthorhombic	orthorhombic	orthorhombic	triclinic
space group	$P\bar{1}$	$Pbca$	$P2_12_12_1$	$P2_12_12_1$	$P\bar{1}$
a [Å]	7.657(3)	7.6722(16)	9.561(4)	9.609(6)	8.700(3)
b [Å]	8.413(3)	13.827(3)	11.781(5)	12.090(7)	10.292(3)
c [Å]	15.951(7)	33.483(7)	24.017(9)	24.349(15)	15.972(5)
α [deg]	91.103(8)	90	90	90	81.354(7)
β [deg]	90.002(9)	90	90	90	74.841(6)
γ [deg]	110.391(8)	90	90	90	73.947(7)
V [Å^3]	963.0(7)	3552.0(13)	2705.3(18)	2829(3)	1321.9(8)
Z	2	8	4	4	2
ρ [Mg m^{-3}]	1.753	1.848	1.419	1.461	1.490
μ(Mo Kα) [mm^{-1}]	2.786	3.019	0.623	1.914	0.644
cryst size [mm^3]	0.21 × 0.07 × 0.02	0.31 × 0.09 × 0.03	0.28 × 0.14 × 0.07	0.30 × 0.14 × 0.10	0.50 × 0.18 × 0.02

dx.doi.org/10.1021/ic2022984 | Inorg. Chem. 2012, 51, 2984−2996

Table 2. continued

	3e	3f	4d	4e	5d
$F(000)$	504	1952	1192	1264	608
θ range [deg]	$1.28 \leq \theta \leq 23.29$	$1.22 \leq \theta \leq 25.34$	$1.70 \leq \theta \leq 23.24$	$1.67 \leq \theta \leq 25.31$	$1.33 \leq \theta \leq 23.37$
max/min transm	1/0.811 958	1/0.748 043	1/0.794 661	1/0.707 371	1/0.690 671
reflns collected	6533	26 702	18 037	22 128	5987
indep reflns [R(int)]	2780 [0.0585]	3251 [0.1228]	3880 [0.0328]	5168 [0.0568]	3803 [0.0314]
reflns with $I > 2\sigma(I)$	1681	1811	3549	4055	2778
GOF on F^2	0.912	1.072	0.923	0.947	1.069
params/restraints	237/0	226/0	310/0	311/0	330/0
R1 (on F, $I > 2\sigma(I)$)	0.0412	0.0412	0.0242	0.0342	0.0421
wR2 (on F^2, all data)	0.0866	0.1179	0.0620	0.0751	0.1099
max/min $\Delta\rho$ [e Å^{-3}]	0.455/−0.417	0.798/−0.614	0.327/−0.160	0.764/−0.383	0.526/−0.326
CCDC number	830406	830407	830408	830409	830410

■ ASSOCIATED CONTENT

Supporting Information

Additional synthesis details, figures, and tables. Crystallographic data in CIF format. This material is available free of charge via the Internet at http://pubs.acs.org.

■ AUTHOR INFORMATION

Corresponding Author

*E-mail: dmsj@qi.uva.es. Phone: +34 983 184096. Fax: +34 983 423013.

Notes

The authors declare no competing financial interest.

■ ACKNOWLEDGMENTS

The authors thank the Spanish Ministerio de Ciencia e Innovación (CTQ2009-12111) and the Junta de Castilla y León (VA070A08 and GR Excelencia 125) for financial support. R.G.-R and C.M.A. wish to acknowledge an MEC-FPU grant and a Ramón y Cajal contract.

■ REFERENCES

(1) *Concepts and Models in Bioinorganic Chemistry*; Kraatz, H. B., Metzler-Nolte, N., Eds.; Wiley-VCH: Weinheim, 2006.

(2) (a) Zagermann, J.; Merz, K.; Metzler-Nolte, N. *Organometallics* **2009**, *28*, 5090−5095. (b) Binkley, S. L.; Ziegler, C. J.; Herrick, R. S.; Rowlett, R. S. *Chem. Commun.* **2010**, *46*, 1203−1205. (c) Alberto, R.; Chibli, R.; Schubiger, A. P. *J. Am. Chem. Soc.* **1999**, *121*, 6076−6077. (d) Liu, Y.; Pak, J. K.; Schmutz, P.; Baauwens, P.; Mertens, J.; Knight, H.; Alberto, R. *J. Am. Chem. Soc.* **2006**, *128*, 15996−15997.

(3) (a) Gosh, D.; Pecoraro, V. *Inorg. Chem.* **2004**, *43*, 7902−7915. (b) Doerr, A. J.; McLendon, G. L. *Inorg. Chem.* **2004**, *43*, 7916−7925.

(4) (a) Fedorova, A.; Ogawa, M. Y. *Bioconjugate Chem.* **2002**, *13*, 150−154. (b) Winkler, J. R.; DiBilio, A. J.; Farrow, N. A.; Richards, J. H.; Gray, H. B. *Pure Appl. Chem.* **1999**, *71*, 1753−1764. (c) Ogawa, M. In *Molecular and Supramolecular Photochemistry*; Ramamurty, V., Schanze, K. S., Eds.; Marcel Dekker: New York, 1999; pp 113−150.

(5) Laungani, A. C.; Keller, M.; Slattery, J. M.; Krossing, I.; Breit, B. *Chem.—Eur. J.* **2009**, *15*, 10405−10422. Barooah, N.; Sarma, R. J.; Baruah, J. B. *Eur. J. Inorg. Chem.* **2006**, 2942−2946.

(6) Laungani, A. C.; Slattery, J. M.; Krossing, I.; Breit, B. *Chem.—Eur. J.* **2008**, *14*, 4488−4502.

(7) Si, S.; Bhattacharjee, R. R.; Banerjee, A.; Mandal, T. K. *Chem.—Eur. J.* **2006**, *12*, 1256−1265.

(8) (a) *Bioorganometallics: Biomolecules, Labeling, Medicine*; Jaouen, G., Ed.; Wiley-VCH: Weinheim, 2006. (b) van Staveren, D. R.; Metzler-Nolte, N. *Chem. Rev.* **2004**, *104*, 5931−5985.

(9) (a) Desiraju, G. R. *Angew. Chem., Int. Ed.* **2007**, *46*, 8342−8356. (b) Das, D.; Desiraju, G. R. *Chem.—Asian J.* **2006**, *1*, 231−244. (c) Braga, D.; Brammer, L.; Champness, N. R. *CrystEngComm* **2005**, *7*, 1−19. (d) Braga, D.; Maini, L.; Mazzeo, P. P.; Ventura, B. *Chem.—Eur. J.* **2010**, *16*, 1553−1559. (e) Braga, D.; Grepioni, F.; Maini, L.; Polito, M.; Rubini, K.; Chierotti, M. R.; Gobetto, R. *Chem.—Eur. J.* **2009**, *15*, 1508−1515.

(10) (a) Kirin, S. I.; Kraatz, H.-B.; Metzler-Nolte, N. *Chem. Soc. Rev.* **2006**, *35*, 348−354. (b) Moriuchi, T.; Yoshida, K.; Hirao, T. *J. Organomet. Chem.* **2003**, *668*, 31−34. (c) Hirao, T. *J. Organomet. Chem.* **2009**, *694*, 806−811.

(11) (a) Heinze, K.; Bueno-Toro, D. *Angew. Chem., Int. Ed.* **2003**, *42*, 4533−4536. (b) Heinze, K. *Dalton Trans.* **2002**, 540−547. (c) Heinze, K.; Jacob, V. *Dalton Trans.* **2002**, 2379−2385.

(12) (a) García-Rodríguez, R.; Miguel, D. *Dalton Trans.* **2006**, 1218−1225. (b) Álvarez, C. M.; García-Rodríguez, R.; Miguel, D. *J. Organomet. Chem.* **2007**, *692*, 5717−5726.

(13) Álvarez, C. M.; García-Rodríguez, R.; Miguel, D. *Dalton Trans.* **2007**, 3546−3554.

(14) Qayyum, H.; Herrick, R. S.; Ziegler, C. *Dalton Trans.* **2011**, *40*, 7442−7445.
(15) Herrick, R. S.; Dupont, J.; Wrona, I.; Pilloni, J.; Beaver, M.; Benotti, M.; Powers, F.; Ziegler, C. J. *J. Organomet. Chem.* **2007**, *692*, 1226−1233.
(16) Wang, W.; Spingler, B.; Alberto, R. *Inorg. Chim. Acta* **2003**, *355*, 386−393.
(17) Herrick, R. S.; Wrona, I.; McMicken, N.; Jones, G.; Ziegler, C. J.; Shaw, J. *J. Organomet. Chem.* **2004**, *689*, 4848−4855.
(18) Herrick, R. S.; Ziegler, C. J.; Bohan, H.; Corey, M.; Eskander, M.; Giguere, J.; McMicken, N.; Wrona, I. E. *J. Organomet. Chem.* **2003**, *687*, 178−184.
(19) The graph notation is used as described in the following references: (a) Berstein, J.; Davis, R. E.; Shimoni, L.; Chang, N. L. *Angew. Chem., Int. Ed.* **1995**, *34*, 1555−1573. (b) Etter, M. C. *Acc. Chem. Res.* **1990**, *23*, 120−126.
(20) Eliel, E. L.; Wilen, S. H. *Stereochemistry of Organic Compounds*; Wiley: New York, 1994.
(21) The chirality is defined by describing the chirality of a triangular face with the metal held remote from the viewer and assigning priorities to the three ligands (halogen and the two nitrogen atoms) according to the Cahn−Ingold−Prelog system, as in the following: Faller, J. W.; Haitko, D. A.; Adams, R. D.; Chodosh, D. F. *J. Am. Chem. Soc.* **1979**, *101*, 865−876.
(22) (a) Toth, K.; Richard, J. P. *J. Am. Chem. Soc.* **2007**, *129*, 3013−3021. (b) Dixon, J. E.; Bruice, T. C. *Biochemistry* **1973**, *12*, 4762−4766.
(23) Espinet, P.; Hernando, R.; Iturbe, G.; Villafañe, F.; Orpen, A. G.; Pascual, I. *Eur. J. Inorg. Chem.* **2000**, 1031−1038.
(24) (a) Cook, J. L.; Hunter, C. A.; Low, C. M. R.; Pérez-Velasco, A.; Vinter, J. M. G. *Angew. Chem., Int. Ed.* **2007**, *46*, 3706−3709. (b) Cook, J. L.; Hunter, C. A.; Low, C. M. R.; Pérez-Velasco, A.; Vinter, J. M. G. *Angew. Chem., Int. Ed.* **2008**, *47*, 6275−6277. (c) Hunter, C. A. *Angew. Chem., Int. Ed.* **2004**, *43*, 5424−5439.
(25) Konrat, R.; Tollinger, M.; Kontaxis, G.; Krautler, B. *Monatsh. Chem.* **1999**, *130*, 961.
(26) Cabrita, E. J.; Berger, S. *Magn. Reson. Chem.* **2001**, *39*, S142−S148.
(27) *SAINT+. SAX Area Detector Integration Program, Version 6.02*; Bruker AXS, Inc.: Madison, WI, 1999.
(28) Sheldrick, G. M. *SADABS, Empirical Absorption Correction Program*; University of Göttingen: Göttingen, Germany, 1997.
(29) Burla, M. C.; Camalli, M.; Carrozzini, B.; Cascarano, G. L.; Giacovazzo, C.; Polidory, G.; Spagna, R. SIR2002, A program for automatic solution and refinement of crystal structures. *J. Appl. Cryst.* **2003**, *36*, 1103.
(30) Farrugia, L. J. *J. Appl. Crystallogr.* **1999**, *32*, 837−838.
(31) Sheldrick, G. M *Acta Crystallogr.* **2008**, *A64*, 112−122. Sheldrick, G. M. *SHELXTL, An Integrated System for Solving, Refining, and Displaying Crystal Structures from Diffraction Data, Version 5.1*; Bruker AXS, Inc.: Madison, WI, 1998.
(32) (a) Nardelli, M. *Comput. Chem.* **1983**, *7*, 95−97. (b) Nardelli, M. *J. Appl. Crystallogr.* **1995**, *28*, 659.
(33) *MERCURY*: (a) Bruno, I. J.; Cole, J. C.; Edgington, P. R.; Kessler, M. K.; Macrae, C. F.; McCabe, P.; Pearson, J.; Taylor, R. *Acta Crystallogr.* **2002**, *B58*, 389−397. (b) Macrae, C. F.; Edgington, P. R.; McCabe, P.; Pidcock, E.; Shields, G. P.; Taylor, R.; Towler, M.; van de Streek, J. *J. Appl. Crystallogr.* **2006**, *39*, 453−457.